HHS Public Access

Author manuscript

J Mol Endocrinol. Author manuscript; available in PMC 2016 January 15.

Published in final edited form as:

J Mol Endocrinol. 2012 October ; 49(2): 79–96. doi:10.1530/JME-12-0028.

Combined blockade of signalling pathways shows marked anti-tumour potential in phaeochromocytoma cell lines

Svenja Nölting[1], **Edwin Garcia**[1], **Ghassan Alusi**[2], **Alessio Giubellino**[3], **Karel Pacak**[3], **Márta Korbonits**[1], and **Ashley B Grossman**[1,4]

[1]Department of Endocrinology, William Harvey Research Institute, Queen Mary University of London, London, UK

[2]Barts Cancer Institute, Barts and the London School of Medicine, Queen Mary University of London, London, UK

[3]NIH, Bethesda, Maryland, USA

[4]Oxford Centre for Diabetes, Endocrinology and Metabolism, Churchill Hospital, University of Oxford, Oxford, UK

Abstract

Currently, there is no completely effective therapy available for metastatic phaeochromocytomas (PCCs) and paragangliomas. In this study, we explore new molecular targeted therapies for these tumours, using one more benign (mouse phaeochromocytoma cell (MPC)) and one more malignant (mouse tumour tissue (MTT)) mouse PCC cell line –both generated from heterozygous neurofibromin 1 knockout mice. Several PCC-promoting gene mutations have been associated with aberrant activation of PI3K/AKT, mTORC1 and RAS/RAF/ERK signalling. We therefore investigated different agents that interfere specifically with these pathways, including antagonism of the IGF1 receptor by NVP-AEW541. We found that NVP-AEW541 significantly reduced MPC and MTT cell viability at relatively high doses but led to a compensatory up-regulation of ERK and mTORC1 signalling at suboptimal doses while PI3K/AKT inhibition remained stable. We subsequently investigated the effect of the dual PI3K/mTORC1/2 inhibitor NVP-BEZ235, which led to a significant decrease of MPC and MTT cell viability at doses down to 50 nM but again increased ERK signalling. Accordingly, we next examined the combination of NVP-BEZ235 with the established agent lovastatin, as this has been described to inhibit ERK signalling. Lovastatin alone significantly reduced MPC and MTT cell viability at therapeutically relevant doses and inhibited both ERK and AKT signalling, but increased mTORC1/p70S6K signalling. Combination treatment with NVP-BEZ235 and lovastatin showed a significant additive effect in MPC and MTT cells and resulted in inhibition of both AKT and mTORC1/p70S6K signalling without ERK up-regulation. Simultaneous inhibition of PI3K/AKT, mTORC1/2 and ERK signalling suggests a novel therapeutic approach for malignant PCCs.

Correspondence should be addressed to A B Grossman who is now at Department of Endocrinology, Oxford Centre for Diabetes, Endocrinology and Metabolism, Churchill Hospital, University of Oxford, Oxford OX3 7LE, UK; ashley.grossman@ocdem.ox.ac.uk.

Declaration of interest

Prof. A B G has received lecture fees and advisory board honoraria from Novartis. Dr S N has received travel costs from Ipsen for attending the ENEA Workshop on Aggressive Pituitary Tumours in Munich, 2011.

Introduction

Most of the phaeochromocytomas (PCCs) are benign neoplasms, but when malignant they can be difficult to treat. This equally applies to extra-adrenal PCCs, better referred to as paragangliomas (PGLs), as recently reviewed (Druce *et al*. 2009, Grogan *et al*. 2011). In such tumours, conventional chemotherapy is usually done with cyclophosphamide, vincristine and doxorubicin (CVD), but even with this treatment, it is difficult to demonstrate any effect on overall survival. If such tumours show uptake of the radiopharmaceutical ^{123}I-metaiodobenzylguanidine (^{123}I-MIBG), then therapy with ^{131}I-MIBG is possible and may have positive therapeutic effects, but tumour regression is not frequently seen. Thus, there is a considerable clinical need for new effective therapies.

One therapeutic approach is to define the aberrant molecular pathways in such tumours, which can then be targeted by therapy. In recent years, an increasing understanding of the germline mutations leading to PCC and PGL development has provided us with crucial insights into the molecular pathology of these tumours (Nölting & Grossman 2012). Indeed, a recent gene profiling study demonstrated a genetic cause, germline or somatic, in 45·5% of these tumours (Burnichon *et al*. 2011). Molecular profiling and analysis have shown that PCCs and PGLs can be separated into two major groups (clusters) according to their transcriptional pattern and underlying gene mutation(s) and appear to follow two separate routes to tumourigenesis, clusters 1 and 2 (Viskochil *et al*. 1990, Latif *et al*. 1993, Mulligan *et al*. 1993, Baysal *et al*. 2000, Niemann & Muller 2000, Astuti *et al*. 2003, Eisenhofer *et al*. 2004, Dahia *et al*. 2005*a*,*b*, Powers *et al*. 2007, Ladroue *et al*. 2008, Schlisio *et al*. 2008, Yeh *et al*. 2008, Hao *et al*. 2009, Burnichon *et al*. 2010, 2011, Favier & Gimenez-Roqueplo 2010, Lopez-Jimenez *et al*. 2010, Qin *et al*. 2010, Comino-Mendez *et al*. 2011). Cluster 1 is related to the Krebs cycle modulation of hypoxia signalling, i.e. to mutations in succinate dehydrogenase subunit A(AF2)/B/C/D (*SDHA*(*AF2*)/*B*/*C*/*D*), the gene associated with von Hippel–Lindaudisease(*VHL*)or2-oxoglutarate-dependent prolyl hydroxylase (*PHD2*); cluster 2 is associated with kinase signalling pathways (PI3K/AKT, RAS/RAF/ERK and mTORC1/p70S6K) and neuroendocrine differentiation and comprises mutations in the rearranged during transfection gene (*RET* that encodes a receptor tyrosine kinase and is associated with multiple endocrine neoplasia type 2 (MEN2)), neurofibromin 1 (*NF1*), kinesin family member 1Bb (*KIF1Bb*) or the recently discovered transmembrane protein 127 (*TMEM127*) and MYC associated factor X (*MAX*). As a common end point, these cluster 2-related mutations are directly or indirectly associated with hyper-phosphorylation of mTORC1 targets (Dahia *et al*. 2005*a*, Qin *et al*. 2010); mTORC1 is a complex consisting of mTOR, the regulatory-associated protein of mTOR (raptor), PRAS40 and mLST8. In addition, cluster 1 changes result in stabilisation and activation of HIF-a, which is also a downstream effector of mTORC1. Thus, signalling pathways converging on mTORC1/2 are attractive candidates for therapeutic manipulation.

In a small number of studies, the growth factor tyrosine kinase inhibitor sunitinib has shown some efficacy in the therapy of malignant PCCs and PGLs, as previously reviewed (Adjalle *et al*. 2009, Fassnacht *et al*. 2009, Joshua *et al*. 2009, Park *et al*. 2009, Santarpia *et al*. 2009). However, the mTORC1 inhibitor everolimus (RAD001, Novartis), which was evaluated in a small number of patients with progressive malignant PGL/PCCs, showed a disappointing

outcome: disease progression was seen in all patients (Druce *et al*. 2009). This low efficacy of single mTORC1 inhibition may have been due to a compensatory activation of the PI3K/AKT signalling pathway by phosphorylation of AKT on Ser473 by mTORC2 (comprising mTOR and the rapamycin-insensitive components of mTOR (rictor), Sin1, mLST8 and protein associated with rictor (protor)) (Hresko & Mueckler 2005, O'Reilly *et al*. 2006, Carracedo & Pandolfi 2008). Compensatory ERK activation via a PI3K-dependent feedback loop has also been described in response to single mTORC1 inhibition (Carracedo *et al*. 2008, Serra *et al*. 2011). These earlier studies suggest that single-agent approaches to malignant PCCs/PGLs are unlikely to be effective in the long term. Accordingly, we have been searching for an effective therapeutic agent or drug combination for the treatment of metastatic PCCs/PGLs among the evolving molecular targeted kinase inhibitors and have especially investigated the potential escape mechanisms of the cell and how these mechanisms of resistance may be prevented. For this purpose, we used two mouse PCC cell lines generated from heterozygous *Nf1* knockout mice (Powers *et al*. 2000, 2007, Martiniova *et al*. 2009). One of the cell lines was more benign (mouse phaeochromocytoma cells (MPCs)) and one more was malignant (mouse tumour tissue derived (MTT)) regarding metastatic spread after reinjection in mice. In terms of therapy, we have used several different agents that interfere with signalling in these cells, including antagonism of the insulin-like growth factor 1 receptor (IGF1 receptor), a receptor tyrosine kinase known to be expressed in these cell lines and human tumours (Fottner *et al*. 2006), and those that block specific signalling cascades such as the mTORC1/2, PI3K/AKT and ERK pathways.

Materials and methods

Reagents

Everolimus, NVP-AEW541 and NVP-BEZ235 were kindly provided by Novartis Pharma. Lovastatin (mevinolin) was purchased from Sigma (M2147). Everolimus blocks mTORC1; NVP-AEW541 is a specific antagonist of the IGF1 receptor; NVP-BEZ235 antagonises both mTORC1/2 and PI3K; lovastatin blocks ERK1/2, AKT, VEGF and EGF receptor functions. For cell culture work, all drugs were diluted in DMSO (10 mM stock solution; Sigma, D8418), which was also used at the appropriate dilution as the vehicle (control) and shown to be equivalent to the blank control up to concentrations of 0·4% DMSO (equivalent to 40 μM drug concentration) in the MTS assay. At drug concentrations higher than 40 μM, MTS assay results are compared to the appropriate vehicle.

Cell culture

Two mouse phaeochromocytoma cell lines, MPC 4/30 PRR mouse phaeochromocytoma cells (MPCs; Powers *et al*. 2000) and mouse tumour tissue-derived (MTT; MTT-derived, more aggressive; Martiniova *et al*. 2009), were kindly provided by Dr Karel Pacak (NIH, Bethesda, MD, USA) and cultured in DMEM medium (Sigma, D6429) containing 10 ml/100 ml foetal bovine serum (FBS; Biosera, FB-1090/500, Labtech International, East Sussex, UK) and 50 units/ml penicillin/50 μg/ml streptomycin (Sigma, P4458) at 37 °C in a 5% CO_2 atmosphere. Both cell lines have been generated from heterozygous *Nf1* knockout mice (Powers *et al*. 2000, Martiniova *et al*. 2009).

Assessment of cell viability

MPC and MTT cells were plated in 96-well plates (Cellstar, 655 180, Greiner Bio-One, Stonehouse –Gloucestershire, UK) in a final volume of 200 µl at a density of 20 000–40 000 cells/well and grown for 24 h. Afterwards, cells were treated with various concentrations of NVP-AEW541, NVP-BEZ235, everolimus or lovastatin, or a combination of NVP-BEZ235 and NVP-AEW541 or a combination of NVP-BEZ235 and lovastatin, for different incubation periods (24, 48 and 72 h) in DMEM medium containing 10 ml/100 ml FBS and 50 units/ml penicillin/50 µg/ml streptomycin. Metabolic activity was assessed by CellTiter 96 AQ_{ueous} One Solution Cell Proliferation Assay (MTS, Promega, G3580) after different incubation times. Following 4 h of incubation with CellTiter 96 AQ_{ueous} One Solution Reagent (20 µl/well), the absorbance at 490 nm was recorded using a 96-well plate reader (Wallac Victor^2, Biodirect, Taunton, MA, USA). For each MTS experiment, eight (n=8) independent samples per group (per time point and drug dose) have been analysed; each MTS experiment was repeated at least two times in an independent manner and, where appropriate, the results of both MTS experiments were taken together (n=8–16). All MTS assay cell viability results are shown as optical density units (ODU, mean±S.E.M.), which are linearly correlated with the cell number (R^2=0·97). For the two drugs, NVP-BEZ235 and lovastatin, as well as for the combination of both drugs, MTS data are shown in two complementary ways – as ODU (mean±S.E.M.) and as the percentage of viable cells (mean ±S.E.M.) compared to the control.

Protein extraction and western blotting

For drug treatment, cells were grown in 75 cm^2 cell culture flasks (Cellstar, 658 175, Greiner Bio-One) in DMEM medium containing 10 ml/100 ml FBS and 50 units/ml penicillin/50 µg/ml streptomycin until they were 80% confluent and, after two washes in PBS (Sigma, D8662), treated with NVP-AEW541, NVP-BEZ235 or lovastatin or a combination of NVP-BEZ235 and lovastatin for the indicated concentration and time in a total volume of 10 ml DMEM containing 10 ml/100 ml FBS and 50 units/ml penicillin/50 µg/ml streptomycin (for treatment with NVP-AEW541) or serum-free DMEM with 50 units/ml penicillin/50 µg/ml streptomycin (for treatment with NVP-BEZ235 or lovastatin or the combination of both drugs). The cells were subsequently washed two times in PBS and scraped into 150 µl phosphosafe lysis buffer (PhosphoSafe Extraction Reagent (Novagen, 71296-4, VWR International, Leicestershire, UK) containing one complete protease inhibitor cocktail tablet per 25 ml (Roche Diagnostics, 11836145001)). Next, lysates were centrifuged at 15 000 ***g*** for 20 min at 4 °C; supernatants were removed and assayed for total protein quantification by Bio-Rad Protein Assay (Bio-Rad, 500-0006, Bio-Rad Laboratories) using BSA (Fisher BioR-eagents, BPE9703-100, Fisher Scientific, Leicestershire, UK) for the standard. Equal amounts of protein (20–75 µg) were denatured in SDS sample buffer, separated on NuPage 10% Bis–Tris Gel (Novex/Invitrogen, NP0301BOX, Life Technologies) and electrophoretically transferred onto a Hybond-P PVDF membrane (Amersham, RPN303F, GE Healthcare, Buckinghamshire, UK). The membrane was blocked in 0·5 g/10 ml skimmed milk powder (for total protein, chromogranin A (CgA) or β-actin) or in 0·5 g/10 ml BSA (for phospho(p)-protein) in TBS/Tween 20 for 1 h at room temperature. Next, the membrane was incubated with the primary antibody (Table 1) diluted

in 0·5 g/10 ml skimmed milk powder (total protein, CgA or β-actin) or in 0·5 g/10 ml BSA (p-protein) in TBS/Tween 20 overnight at 4 °C. After three washes in TBS/Tween 20, the membrane was incubated with the secondary antibody (Table 1) in 0·5 g/10 ml skimmed milk powder in TBS/Tween 20 for 1 h at room temperature followed by two washes in TBS/Tween 20 and one wash in TBS without Tween. Immunodetection was performed using the Odyssey infrared imaging system (LI-COR, Biosciences, Cambridge, UK). Each membrane was incubated and double stained with two primary antibodies (p-protein and total protein or CgA and β-actin). Cross-detection between analysed proteins was avoided using different species raised against primary antibodies. The optical density of the approximately sized bands was measured using the Odyssey molecular imaging software (LI-COR Biosciences). The relative expression of each p-protein was calculated as the ratio of p-/total protein ODU (mean±S.E.M.). CgA was normalised to β-actin and calculated as a ratio of CgA/β-actin ODU (mean±S.E.M.). For each western blot experiment, three (n=3) to four (n=4) independent samples per group (per time point and drug dose) have been analysed; each western blot experiment was repeated at least two times in an independent manner and, where appropriate, the results of both western blot experiments were taken together for the western blot graphs (usually n=6–7).

Assessment of apoptosis

Caspase-Glo 3/7 assay—MPC and MTT cells were plated in white-walled 96-well plates (Costar, 3610, Corning, Corning, NY, USA) in a final volume of 100 µl at a density of 20 000 cells/well and grown for 24 h. Afterwards, cells were treated with NVP-BEZ235 or lovastatin or the combination of both drugs for the indicated concentration and time in DMEM containing 10 ml/100 ml FBS and 50 units/ml penicillin/50 µg/ml streptomycin. Apoptosis was measured by Caspase-Glo 3/7 Assay (Promega, G8091). After dissolving the lyophilised caspase substrate in the caspase buffer, 100 µl of reagent was added to each well in the white-walled 96-well plates. After 0·5 h, the caspase activity was measured by luminescence using a 96-well plate reader (Wallac Victor^2, Biodirect). Eight (n=8) independent samples per group (per time point and drug dose) have been analysed; the results are shown as ODU (mean±S.E.M.).

Flow cytometry: PE Active Caspase-3 Apoptosis Kit—MPC and MTT cells were plated at a density of $2{\cdot}5\times10^5$ cells/well in six-well plates (Cellstar, 657 160, Greiner Bio-One) in a final volume of 2 ml DMEM medium containing 10 ml/100 ml FBS and 50 units/ml penicillin/50 µg/ml streptomycin and were grown for 24 h. Afterwards, cells were treated with NVP-BEZ235 or lovastatin or the combination of both drugs for the indicated concentration and time. Apoptosis was measured by flow cytometry using the PE Active Caspase-3 Apoptosis Kit (BD Pharmingen, 550914, BD Biosciences, San Diego, CA, USA). Briefly, after the indicated incubation time, cells were washed once in PBS, harvested by gentle trypsinisation, centrifuged at 1500 ***g*** for 5 min and washed again twice in cold PBS. Next, each test was resuspended in 0·5 ml BD Cytofix/Cytoperm solution. Following 20 min of incubation on ice, cells were centrifuged at 1200 ***g*** for 5 min, washed twice in 0·5 ml BD Perm/Wash per sample and resuspended in 100 µl BD Perm/Wash plus 20 µl PE Rabbit Anti-Active Caspase-3 Antibody (BD Pharmingen, 51-68655X, BD Biosciences) per sample. After 30 min of incubation at room temperature, each test was washed again in 1 ml

BD Perm/Wash and resuspended in 0·5 ml BD Perm/Wash. Data were collected on a FACSCalibur flow cytometer (BD Biosciences) using CellQuest software (BD Biosciences), and quantitative analysis was performed using FlowJo analytical software (Tree Star, Ashland, OR, USA). Each experiment was repeated two times in an independent manner.

Cell cycle analysis by flow cytometry

MPC and MTT cells were plated at a density of 3×10^5 cells/well in six-well plates (Cellstar, 657 160, Greiner Bio-One) in a final volume of 2 ml DMEM medium containing 10 ml/100 ml FBS and 50 units/ml penicillin/50 μg/ml streptomycin and grown for 24 h. Afterwards, cells were treated with NVP-BEZ235 or lovastatin or the combination of both drugs for the indicated concentration and time. After the indicated incubation time, cells were washed once in PBS, harvested by gentle trypsinisation, centrifuged at 1500 ***g*** for 5 min and washed once again in cold PBS. Next, each test was resuspended in 0·5 ml of cold 70% ethanol. After 30 min of incubation at 4 °C, the cells were washed once in cold PBS and resuspended in PBS containing 50 μg/ml propidium iodide (Sigma, P4170) and 100 μg/ml RNAse (Sigma, R4642). After 30 min of incubation in the dark at room temperature, cell counts were taken using a FACSCalibur flow cytometer (BD Biosciences) using CellQuest software (BD Biosciences) and quantitative analysis was performed using FlowJo analytical software (Tree Star). Each experiment was repeated two times in an independent manner.

Statistical analysis

Statistical analysis was performed with GraphPad Prism (GraphPad Software, La Jolla, CA, USA). Cell viability assay (MTS) and caspase assay data were noted to be normally distributed (Kolmogorov–Smirnov test) and were statistically analysed by one-way ANOVA followed by Turkey's multiple comparison test. Western blot data were not normally distributed and were analysed by the Mann–Whitney test. Statistical significance was defined at $P\leq0{\cdot}05$. Data are shown as mean±S.E.M.

Results

Treatment with NVP-AEW541 dose- and time-dependently decreased MPC and MTT cell viability

MPC and MTT cells were treated with 10 nM–100 μM NVP-AEW541 for 24–72 h and cell viability was assessed by MTS assay. Treatment of MPC and MTT cells with NVP-AEW541 for 48 h significantly decreased cell viability at doses of 1 and 4 μM, respectively, and at higher concentrations compared with the control ($P\leq0{\cdot}001$; Fig. 1A). In MTT cells, this effect was already seen at 24 h, with a persistent and slightly stronger effect after 72 h (Fig. 1B). Similar data were found in MPC cells (ODU after 24 h: control (n=8) vs 10 μM NVP-AEW541 (n=8): 1·34±0·03 vs 0·69±0·02, $P\leq0{\cdot}001$; ODU after 72 h: control (n=8) vs 10 μM NVP-AEW541 (n=8): 1·70±0·05 vs 0·55±0·01, $P\leq0{\cdot}001$).

However, relatively high doses of NVP-AEW541 were needed to show a significant effect on cell viability. We therefore proceeded to investigate the possible mechanism of relative resistance of the cells to lower doses of the IGF1 receptor inhibitor and studied the regulatory pathways at a suboptimal dose of 6 μM after 24 h treatment in MTT cells. Our

results showed that, while there was a decreased phosphorylation of AKT at this dose, there was an increased phosphorylation of ERK and p70S6K compared with the vehicle (Fig. 1C). The stimulation of ERK observed in the cell lines was lost at high doses of NVP-AEW541, although the stimulation of p70S6K persisted.

The significant increase in pERK and pp70S6K accompanying a significant decrease in pAKT after NVP-AEW541 treatment suggested that multiple pathways need to be antagonised to provide a robust inhibition of proliferation. Therefore, we further investigated the effect of the novel dual PI3K/mTORC1/2 inhibitor NVP-BEZ235 in both cell lines.

Treatment with NVP-BEZ235 dose- and time-dependently decreased MPC and MTT cell viability

Treatment for 24, 48 and 72 h with NVP-BEZ235 significantly and progressively more potently decreased MPC cell viability compared with the control ($P \leq 0{\cdot}001$; Fig. 2A). These effects were seen at doses down to 50 nM. The cell viability curves for MPC cells are shown in Fig. 2B. NVP-BEZ235 treatment for 24, 48 and 72 h also significantly decreased MTT cell viability at doses down to 50 nM ($P \leq 0{\cdot}001$) (ODU after 24 h: control (n=8) vs 50 nM NVP-BEZ235 (n=8): 0·94±0·02 vs 0·74±0·02, $P \leq 0{\cdot}001$; ODU after 48 h: control (n=8) vs 50 nM NVP-BEZ235 (n=8): 1·36±0·06 vs 0·99±0·03, $P \leq 0{\cdot}001$; ODU after 72 h NVP-BEZ235: control (n=16) vs 50 nM NVP-BEZ235 (n=12): 1·47±0·08 vs 0·78±0·08, $P \leq 0{\cdot}001$). Treatment with 1 and 10 μM NVP-BEZ235 for 48 h decreased MTT cell viability by 87 and 100%, respectively, compared with the control. Treatment with 1 and 10 μM NVP-BEZ235 for 72 h reduced MTT cell viability by 98 and 100%, respectively, compared with the control. Treatment of MPC cells with 100 nM NVP-BEZ235 for 24 h significantly decreased pAKT and pp70S6K levels but significantly increased pERK levels compared with the vehicle (Fig. 2C).

As a typical biochemical marker, chromaffin cells of the adrenal medulla contain CgA, which is co-released with adrenaline and noradrenaline from the secretory dense core granules. Therefore, CgA expression is a useful tool to prove the neuroendocrine characteristics of PCC cells. CgA is the best existing tumour marker for neuroendocrine tumours (NETs) in general and is also especially a good clinical marker for PCCs and PGLs with an association with malignancy and tumour load. Moreover, alterations in CgA level may be useful clinical predictors of treatment success. Therefore, we further investigated the influence of this drug showing efficacy *in vitro* on CgA protein levels. We detected both 50 and 71 kDa fragment of CgA in both non-treated and treated MPC cells: the protein level of the 50 kDa fragment was significantly diminished, while the 71 kDa fragment remained constant after treatment with 100 nM NVP-BEZ235 for 24 h compared with the vehicle (Fig. 2D).

NVP-BEZ235 compared to everolimus

To see whether the effects of NVP-BEZ235 were mainly related to inhibition of the mTORC1 pathway, we compared its potential with the specific mTORC1 inhibitor, everolimus (Fig. 3). We found that 50–500 nM NVP-BEZ235 and everolimus were broadly similar, although at higher doses (1 μM) NVP-BEZ235 was slightly more effective.

The combination of low doses of NVP-BEZ235 with NVP-AEW541

As both NVP-AEW541 and NVP-BEZ235 led to a decrease in cell viability but there was increased phosphorylation of ERK1/2 in both cases, we speculated that there would be little effect in combining these two agents. Indeed, while there was a statistically significant additive effect in MPC cells after combination treatment with 6 μM NVP-AEW541 and 50 or 100 nM NVP-BEZ235 for 24 h, this was quite modest and the combination was not materially different to each drug separately (ODU after 24 h: control (n=8) vs 6 μM NVP-AEW541 (n=8): 0·85±0·004 vs 0·79±0·01, P≤0·01; control (n=8) vs 50 nM (100 nM) NVP-BEZ235 (n=8): 0·85±0·004 vs 0·79±0·01 (0·78±0·01), P≤0·001; 6 μM NVP-AEW541 (n=8) vs 6 μM NVP-AEW541 plus 50 nM (100 nM) NVP-BEZ235 (n=8): 0·79±0·01 vs 0·72±0·005 (0·71±0·004), P≤0·001; 50 nM (100 nM) NVP-BEZ235 (n=8) vs 6 μM NVP-AEW541 plus 50 nM (100 nM) NVP-BEZ235 (n=8): 0·79±0·01 (0·78±0·01) vs 0·72±0·005 (0·71±0·004), P≤0·001).

Lovastatin as an ERK inhibitor

Lovastatin is an established, safe and well-tolerated drug that has recently been described to have anti-tumour potential and to inhibit both ERK and AKT signalling *in vitro* in different cancer cell lines and *in vivo* in animal models. Consequently, we investigated the effect of lovastatin in both PCC cell lines.

We found that 24 h treatment with lovastatin did not affect MPC (Fig. 4A) or MTT cell viability. However, 48 h treatment with 20 μM lovastatin and 72 h treatment with 5 μM lovastatin significantly decreased MPC cell viability compared with the control (P≤0·001 and P≤0·01 respectively; Fig. 4A). The cell viability curves for MPC cells are shown in Fig. 4B. A significant decrease in MTT cell viability was observed at a dose of 20 μM after 48 h treatment and at a dose of 10 μM after 72 h treatment (ODU after 48 h: control (n=8) vs 20 μM lovastatin (n=8): 1·21±0·04 vs 0·90±0·02, P≤0·001; ODU after 72 h: control (n=8) vs 10 μM lovastatin (n=8): 1·35 ±0·04 vs 1·09±0·04, P≤0·001). Treatment with 40 μM lovastatin for 48 and 72 h decreased MTT cell viability by 79 and 83%, respectively, compared with the control. At doses higher than 40 μM, lovastatin crystallised in FBS-containing media and was therefore cytotoxic.

Treatment of MPC cells with 10 μM lovastatin for 72 h significantly decreased pAKT and pERK but significantly increased pp70S6K compared with the vehicle (Fig. 4C). In addition, both the 50 and 71 kDa fragments of CgA were significantly diminished after treatment with 10 μM lovastatin for 72 h compared with the vehicle (ratio CgA/β-actin: vehicle (n=3) vs 10 μM lovastatin (n=3): 71 kDa fragment of CgA: 0·018±0·0008 vs 0·0073±0·002, P≤0·05; 50 kDa fragment of CgA: 0·003±0·0006 vs 0·0002±0·0001, P≤0·05).

The combination of NVP-BEZ235 and lovastatin

As lovastatin significantly decreased MPC and MTT cell viability and significantly inhibited AKT and ERK signalling, we next investigated whether the combination of lovastatin with NVP-BEZ235 would reveal an additive effect on cell proliferation inhibition. Lovastatin was added 24 h before the combination treatment for 48 h. In MPC cells, we observed a significant additive effect for the combination of 10 μM lovastatin with 50 or 100 nM NVP-

BEZ235 ($P \leq 0{\cdot}001$; Fig. 5A and B). In MTT cells, a significant additive effect was also shown by combining 10 μM lovastatin with 50 nM NVP-BEZ235 (ODU: control (n=8) vs 10 μM lovastatin (n=8): 1·23±0·06 vs 0·88±0·02, $P \leq 0{\cdot}001$; control (n=8) vs 50 nM NVP-BEZ235 (n=8): 1·23±0·06 vs 0·88±0·02, $P \leq 0{\cdot}001$; 10 μM lovastatin (n=8) vs 10 μM lovastatin plus 50 nM NVP-BEZ235 (n=8): 0·88±0·02 vs 0·73±0·02, $P \leq 0{\cdot}05$; 50 nM NVP-BEZ235 (n=8) vs 10 μM lovastatin plus 50 nM NVP-BEZ235 (n=8): 0·88±0·02 vs 0·73 ±0·02, $P \leq 0{\cdot}05$). Single treatment with 10 μM lovastatin for 72 h reduced MTT cell viability by 54% compared with the control. Single treatment with 50 nM NVP-BEZ235 for 48 h also reduced MTT cell viability by 54% compared with the control. Treatment with 50 nM NVP-BEZ235 in combination with 10 μM lovastatin for 48 h decreased MTT cell viability by 77% compared with the control. Pretreat-ment of MPC cells with 10 μM lovastatin for 48 h followed by the addition of 50 nM NVP-BEZ235 for 24 h significantly decreased pAKT and pp70S6K compared with the vehicle and also prevented pERK up-regulation previously induced by the single NVP-BEZ235 treatment (Fig. 5C). Moreover, pretreatment with 10 μM lovastatin for 48 h followed by the addition of 50 nM NVP-BEZ235 for 24 h significantly decreased both the 50 and 71 kDa fragments of CgA in MPC cells compared with the vehicle (Fig. 5D).

Measurement of apoptosis

No apoptosis induction was seen after single NVP-BEZ235 treatment in MTT cells. By contrast, lovastatin treatment significantly increased apoptosis compared with the vehicle. Combination treatment in turn slightly decreased the apoptosis seen with lovastatin treatment alone with increasing doses of NVP-BEZ235 but significantly increased apoptosis compared with single treatment with NVP-BEZ235 (Fig. 6A). These results were confirmed using flow cytometry to assess the percentage of active caspase-3-positive cells; NVP-BEZ235 treatment alone did not induce apoptosis, while lovastatin massively increased apoptosis compared with the vehicle. The combination treatment slightly decreased apoptosis compared with single lovastatin treatment but increased apoptosis compared with NVP-BEZ235 treatment alone. The results for MTT cells are shown in Fig. 6B. MPC cells showed a similar pattern with slightly less apoptosis induction compared with the vehicle after treatment with lovastatin alone and the drug combination (data not shown).

Cell cycle

Lovastatin and NVP-BEZ235 separately decreased the percentage of cells in the S-phase with a marked additive effect when both drugs were combined and concomitantly increased the percentage of cells in the G0/G1-phase. These data indicate that lovastatin and NVP-BEZ235 separately induce cell cycle arrest in the G0/G1 phase with a markedly stronger effect after combination treatment. The data for the MPC cells are shown in Fig. 7, and similar results were found for MTT cells (data not shown).

Discussion

In this study, we have investigated potential novel therapeutic agents for treating malignant PCCs/PGLs: these are at present frequently fatal due to a lack of a completely effective therapy. For this purpose, we used two novel mouse PCC cell lines – one less aggressive

(MPC) and one more aggressive (MTT) (Powers *et al*. 2000, Martiniova *et al*. 2009). There are no human PCC cell lines available at present to study the pathogenesis of PCC and PGL. Therefore, we used two complementary mouse PCC cell lines – MPC and MTT – to investigate new molecular targeted therapy options. While this is probably the most suitable cell line model currently available, it has to be critically considered that both cell lines have been generated on the same genetic NF1 knockout background, which limits the interpretation and generalisation of the data. Therefore, the conclusions made from this study may not be completely transferable to all PCCs/PGLs from different genetic backgrounds, although we would suggest that they may well be applicable to human tumours based on cluster 2 mutations.

Inhibition of IGF1 receptor: NVP-AEW541

The IGF1 receptor is a receptor tyrosine kinase. IGF1 has been reported to be a regulator of NET growth by stimulating PI3K/AKT, RAS/RAF/ERK and mTORC1/p70S6K signalling pathways (von Wichert *et al*. 2000), which are especially altered as a consequence of cluster 2-related PCC/PGL susceptibility gene mutations (Viskochil *et al*. 1990, Mulligan *et al*. 1993, Powers *et al*. 2000, 2007, Dahia *et al*. 2005*a*, Schlisio *et al*. 2008, Qin *et al*. 2010, Burnichon *et al*. 2011, Comino-Mendez *et al*. 2011). Furthermore, *TMEM127*-mutant PCCs, which are transcriptionally related to *NF1*-mutant PCCs, were amongst others enriched in IGF1 receptor signalling pathways (Astuti *et al*. 2003), and the IGF1 receptor has been reported to be over-expressed in human PCCs (Fottner *et al*. 2006). The novel IGF1 receptor inhibitor NVP-AEW541 has been shown to attenuate proliferation in human NET cell lines of midgut, pancreatic and bronchial origin and in primary cultures of human NETs and breast cancer cells by inhibiting PI3K/AKT, RAS/RAF/ERK and mTORC1/p70S6K signalling (Hopfner *et al*. 2006, Serra *et al*. 2008, Zitzmann *et al*. 2010). Therefore, we examined the effect of NVP-AEW541 on PCC cells. Unexpectedly, relatively high doses were needed to show an apparent effect, i.e. at least 2 μM after 72 h treatment of MTT cells. By investigating the mechanism of resistance of the cell at lower drug doses, we found that a sustained inhibition of AKT at suboptimal doses of NVP-AEW541 was accompanied by up-regulation of ERK and mTORC1/p70S6K signalling (relative resistance). Activated AKT can inhibit growth factor-induced RAF activity and RAF/MEK/ERK signalling, possibly explaining the activation of ERK in response to AKT inhibition (Zimmermann & Moelling 1999, Guan *et al*. 2000). ERK activation has previously been described in response to PI3K/AKT inhibition in breast cancer cells and has been suggested as the cause of resistance to IGF1 receptor inhibitor therapy in Ewing sarcoma patients after an initial response (Serra *et al*. 2011, Subbiah *et al*. 2011). The observed mTORC1/p70S6K activation also demonstrates a mechanism of resistance to growth factor receptor blockade. We therefore concluded that there was a need to target multiple signalling pathways to enhance efficacy. Consequently, we further investigated the potential of dual PI3K/mTORC1/2 inhibitor NVP-BEZ235 in both PCC cell lines.

Dual PI3K/mTORC1/2 inhibitor NVP-BEZ235

The dual PI3K/mTORC1/2 inhibitor NVP-BEZ235 showed high anti-tumour potential already at low doses; even 50 nM NVP-BEZ235 led to a significant decrease in MPC and MTT cell viability after 24 h of treatment. Treatment with 100 nM NVP-BEZ235 for 24 h

that significantly inhibited PI3K/AKT and mTORC1/p70S6K signalling, however, led to a significant up-regulation of ERK signalling, which may be considered as a potential mechanism of resistance to this drug. ERK up-regulation in response to NVP-BEZ235 treatment has already been described in human NET cell lines (Zitzmann *et al*. 2010). As another potential mechanism of resistance to low doses of NVP-BEZ235, Serra *et al*. reported activation of AKT signalling in breast cancer cells after 48 h treatment with low doses (10–100 nM) of NVP-BEZ235, mTORC1/p70S6K inhibition remained stable. This AKT activation in breast cancer cells could be prevented by addition of the IGF1 receptor inhibitor NVP-AEW541 in that study (Serra *et al*. 2008). We found sustained AKT inhibition after 24 h treatment with 100 nm NVP-BEZ235. However, in our study, treatment of MPC cells with both NVP-BEZ235 and NVP-AEW541 individually led to an increase in ERK1/2 signalling. We therefore suspected that combining both drugs might have little effect in MPC cells due to an escape mechanism via ERK signalling. Although we were able to show an additive effect of the combination of NVP-BEZ235 with NVP-AEW541 on MPC cell viability, this effect was not remarkably different from each drug separately. Moreover, the similar effect of the single mTORC1 inhibitor everolimus and the dual PI3K/mTORC1/2 inhibitor NVP-BEZ235 at lower doses argued for a greater relative importance of mTORC1 inhibition compared with a modest effect of additional AKT inhibition. However, both single mTORC1 inhibition and dual PI3K/mTORC1/2 inhibition have been shown to result in ERK activation (Carracedo *et al*. 2008, Zitzmann *et al*. 2010). Consistent with these findings, breast cancer cells affected by PTEN loss of function or *KRAS* mutations were resistant to NVP-BEZ235, partly due to ERK pathway activity (Brachmann *et al*. 2009). Interestingly, NVP-BEZ235 did not induce apoptosis, which is consistent with the observed ERK up-regulation and the previously reported VEGF up-regulation after NVP-BEZ235 treatment (Zitzmann *et al*. 2010) as ERK activation has been described to prevent apoptosis, for example in traumatic brain injury models via a VEGF-dependent mechanism (Ma *et al*. 2011). Conversely, we found an inhibitory effect on the cell cycle with an induction of G1 arrest after NVP-BEZ235 treatment in MPC and MTT cells. It has also previously been shown in non-functioning pituitary adenoma that NVP-BEZ235 only displayed a cytostatic action, inhibiting cell proliferation with G1-phase cell-cycle arrest but no apoptosis (Lee *et al*. 2011). Accordingly, we concluded that the best additional effect might be achieved by combining dual inhibition of PI3K/mTORC1/2 with an ERK inhibitor.

Lovastatin as an ERK inhibitor

Statins have been reported to have a remarkable anti-tumour potential and induce apoptosis in many cancer cells lines of different origin, as previously summarised (Holstein *et al*. 2006), such as leukaemia, breast, ovarian, cervical, prostate, colon, pancreatic, squamous epithelial, lung, mesothelioma and brain cancer cell lines by inhibiting the PI3K/AKT and ERK signalling pathways as well as VEGF and EGF receptor functions (Mantha *et al*. 2005, Dimitroulakos *et al*. 2006, Cemeus *et al*. 2008, Park *et al*. 2010, Zhao *et al*. 2010). We therefore speculated that lovastatin may be an interesting therapeutic agent for both cluster 1 (*VHL*, *SDHx* and *PHD*, associated with VEGF receptor signalling dysregulation) and cluster 2 (*RET*, *NF1*, *KIF1Bb*, *MAX*, *TMEM127*, related to PI3K/AKT, mTORC1/p70S6K and RAS/RAF/ERK signalling dysregulation) mutated PCCs/PGLs. Statins have never previously been tested in any NET or PCC cell line. Lovastatin is an inhibitor of 3-

hydroxy-3-methylglutaryl-CoA reductase (HMG-CoA reductase). The HMG-CoA reductase pathway is, amongst others, responsible for isoprenylation (geranyl-geranylation and farnesylation respectively) of the RHO and RAS family of G proteins, their localisation to the inner surface of the cell membrane and their function. There are substantial interactions between RHO, RAS and RAC pathways: RHO proteins are typically geranylgeranylated and RAS proteins farnesy-lated, as previously reviewed (Demierre *et al*. 2005). PCC-promoting gene mutations, especially cluster 2 mutations of *RET* and *NF1*, have been associated with constitutive activation of RAS/RAF/ERK signalling, as recently reviewed (Nölting & Grossman 2012). It has previously been shown that lovastatin induces apoptosis in acute myelogenous leukaemia (AML) cells, probably at least in part due to a significant down-regulation of pERK1/2 (Wu *et al*. 2004), consistent with our findings in PCC cells. We also found that lovastatin significantly dose- and time-dependently decreased MPC and MTT cell viability and induced apoptosis, probably in part by inhibiting both ERK and AKT signalling as a possible consequence of lovastatin-induced disruption of RAS or/and RHO signalling. Addition of geranylgeranyl pyrophosphate reversed lovastatin-induced apoptosis and loss of ERK1/2 phosphorylation in AML cells (Wu *et al*. 2004). This may be explained by the fact that RAS proteins can be alternatively geranylgeranylated in the presence of farnesyl protein transferase inhibitors (Whyte *et al*. 1997). Moreover, RHO seems to be necessary for RAS-induced tumourigenesis (Olson *et al*. 1998), and dominant-active RHOA also reversed lovastatin-induced apoptosis and, in part, statin-induced down-regulation of the anti-apoptotic protein BCL2 (Demierre *et al*. 2005). Thus, inhibition of ERK1/2 signalling and induction of apoptosis by lovastatin may be due to a HMG-CoA-dependent mechanism involving loss of isoprenylation of RAS or/and RHO family proteins. It has previously been described that statins induced apoptosis to a greater degree in malignant than in non-malignant cells (Wong *et al*. 2002, Wu *et al*. 2004), possibly because of the higher expression of HMG-CoA reductase in malignant cells and a greater dependence on mevalonate-derived isoprenoids of malignant cells compared with benign cells (Hentosh *et al*. 2001). Accordingly, we also found that lovastatin induced apoptosis to a greater degree in MTT than in MPC cells compared with the vehicle (data not shown). Induction of a constitutively active RAF/MEK/ERK pathway in AML cells significantly repressed, but did not completely abrogate, lovastatin-induced apoptosis (Wu *et al*. 2004). These findings are in agreement with our conclusion that down-regulation of ERK signalling may at least be part of the pro-apoptotic effect of lovastatin. Consistent with our results of increased caspase-3/7 activity after lovastatin treatment, activation of caspases has previously been described to be involved in statin-induced apoptosis (Marcelli *et al*. 1998, Cafforio *et al*. 2005, Follet *et al*. 2012). Cell proliferation inhibition by statins through down-regulation of CDK2, aurora kinases A and B, and cyclins A, B1 and D1 and up-regulation of the cell cycle inhibitors $p21^{CIP1}$ and p27 has also previously been documented. These effects have been found to be both HMG-CoA dependent and HMG-CoA independent (Jakobisiak *et al*. 1991, Crick *et al*. 1998, Rao *et al*. 1999, Park *et al*. 2001, Ukomadu & Dutta 2003, Follet *et al*. 2012). Statins inhibited the cell cycle by the induction of G1/S arrest and/or G2/M arrest in several different cell lines (Maltese & Sheridan 1985, Jakobisiak *et al*. 1991, Crick *et al*. 1998, Park *et al*. 2001). We also found a G1 phase cell cycle arrest after lovastatin treatment in MPC and MTT cells.

While only poorly effective on their own against different malignancies in humans, lovastatin and other statins have been found to remarkably augment the effectiveness of different chemotherapeutics such as doxorubicin, cisplatin, cytosine arabinoside, paclitaxel, 5-fluorouracil and tumour necrosis factor-α (Holstein *et al*. 2006), as well as of VEGF and EGF receptor inhibitors such as gefitinib (Mantha *et al*. 2005, Dimitroulakos *et al*. 2006, Cemeus *et al*. 2008, Park *et al*. 2010, Zhao *et al*. 2010). The previously reported poor efficacy of single lovastatin treatment in different malignancies in humans may in part be explained by the increase in mTORC1/p70S6K signalling after lovastatin treatment, as observed in this study. The lovastatin doses needed to show a significant effect on PCC cell viability (5 and 10 μM for 72 h, respectively, in MPC and MTT cells) are not exceptionally high compared with other cell lines treated with lovastatin and may be therapeutically relevant (plasma lovastatin bioactivity levels up to 12·3 μM are achievable in humans without reaching a dose-limiting toxicity; Holstein *et al*. 2006). In the majority of cell lines, doses of 5–30 μM lovastatin for 36–96 h were required to induce apoptosis (Holstein *et al*. 2006). Similar high doses were needed for the RAF1 inhibitor Raf265 to show an effect in three different human NET cell lines (Zitzmann *et al*. 2010).

Consistent with our conclusion that ERK1/2 inhibition by lovastatin is at least partly responsible for apoptosis induction in PCC cells, Zitzmann *et al*. (2010) also showed a significant decrease in cell viability, inhibition of cell proliferation and induction of apoptosis in human midgut (GOT), pancreatic (BON) and broncho-pulmonary (H727) NET cell lines through RAF/MEK/ERK1/2 pathway inhibition with the RAF1 inhibitor RAF265: interestingly, there was no correlation between measured basal ERK activity and sensitivity to RAF265. In several other solid tumours such as breast and prostate cancer (Carracedo *et al*. 2008, Kinkade *et al*. 2008) and in leukaemia (Steelman *et al*. 2008), RAF/MEK/ERK pathway inhibition, especially in combination with mTOR inhibition, has also been found to have crucial anti-tumour potential (Grant 2008, Ricciardi *et al*. 2012). Moreover, it has recently been reported that generation of reactive oxygen species and downstream activation of RAS/RAF/ERK and RAS/PI3K pathways by silibinin could prevent apoptosis in PCC (PC12) cells (Liu *et al*. 2011). As discussed in detail earlier, lovastatin has already been postulated to induce apoptosis at least in part through ERK1/2 inhibition, as constitutively active RAF/MEK/ERK signalling significantly repressed lovastatin-induced apoptosis (Wu *et al*. 2004). By contrast, it has been reported that RAF1 activation led to a significant decrease in secretion from medullary thyroid carcinoma cells (decrease of CgA and calcitonin), human pancreatic (BON) and human pulmonary (H727) NET cells (Sippel & Chen 2002, Sippel *et al*. 2003*a*,*b*, Cook *et al*. 2010). Interestingly, this effect could be inhibited by MEK inhibitors that, however, did not influence ERK1/2 phosphorylation, implicating an ERK1/2-independent pathway (Sippel *et al*. 2003*a*,*b*). While Sippel *et al*. (2003*b*) found that RAF1 activation did not to influence human pancreatic (BON) NET cell growth, other studies suggested that the RAF1 activator ZM336372 (as well as the drugs leflunomide and teriflunomide – both also associated with RAF1 pathway activation) suppressed the growth of human pulmonary (H727) and human pancreatic (BON) NET cells *in vitro*; for leflunomide and teriflunomide, this was also shown *in vivo* (Van Gompel *et al*. 2005, Cook *et al*. 2010). The *in vivo* reduction in development and growth of human medullary thyroid carcinomas through RAF1 activation has also been reported (Vaccaro *et*

al. 2006). Moreover, 100 μM and higher doses of the RAF1 activator ZM336372 have been reported to significantly decrease PCC (PC12) cell viability (Kappes *et al*. 2006). Nevertheless, at an effective dose of 100 μM ZM336372, no ERK1/2 up-regulation could be detected by western blotting. While at a dose of 200 μM a strong increase in ERK1/2 phosphorylation was detected, ERK1/2 phosphoryl-ation slightly decreased again at a higher dose of 300 μM (Kappes *et al*. 2006). Thus, in this case, other signalling pathways may be involved in the anti-tumour potential of this drug. Interactions between the PI3K, mTORC1/2 and the RAF/MEK/ERK pathway have already been described (Grant 2008, Nölting & Grossman 2012). Therefore, interactions of these pathways must also be considered. Indeed, mTORC1 inhibition has been reported to lead to RAF/MEK/ERK pathway activation (Carracedo *et al*. 2008). In these and other studies (Zitzmann *et al*. 2010), the dual PI3K/mTORC1/2 inhibitor NVP-BEZ235 displayed anti-tumour potential and, at the same time, led to ERK1/2 up-regulation. However, additional RAF1/MEK/ERK1/2 pathway inhibition by the RAF1 inhibitor RAF265 enhanced its anti-tumour potential in three different human NET cell lines (BON, H727 and GOT; Zitzmann *et al*. 2010). Moreover, synergistic anti-tumour effects of the mTORC1 inhibitor RAD001 and MEK inhibitors have very recently been reported in two different human NET cell lines (H727 and COLO320; Iida *et al*. 2012). Therefore, the critical role of RAF/MEK/ERK1/2 activation should be regarded, especially in the context of resistance to PI3K or/and mTORC1/2 inhibitors. In summary, both induced up-regulation and inhibition of the RAF/MEK/ERK signalling pathway may disturb ‘optimally balanced’ basal ERK activity in the tumour cell and lead to a decrease in cell viability. However, it may be therapeutically important to at least prevent the endogenous ‘compensatory’ ERK up-regulation of the tumour cell in response to PI3K or/and mTORC1/2 inhibitors and avoid this possible mechanism of resistance.

Combination of lovastatin and NVP-BEZ235

Pretreatment with 5 and 10 μM lovastatin, respectively, for 24 h has recently been shown to inhibit VEGF and EGF receptor signalling *in vitro* (by inhibiting ligand-binding-induced endocytosis), thus leading to compensatory up-regulation of VEGF and EGF receptors making tumour cells *in vitro* more susceptible to VEGF and EGF receptor inhibition by tyrosine kinase inhibitors such as gefitinib (Dimitroulakos *et al*. 2006, Holstein *et al*. 2006, Zhao *et al*. 2010). Therefore, we used the same treatment conditions and pretreated MPC and MTT cells for 24 h with lovastatin followed by combination treatment with lovastatin and NVP-BEZ235 for 48 h; we found that combination treatment showed a significantly stronger effect than each drug separately, probably due to the significant inhibition of PI3K/AKT and mTORC1/p70S6K signalling and the loss of ERK up-regulation. Consistent with these findings, it has previously been reported that lovastatin can overcome gefitinib resistance in *KRAS*-mutated non-small cell lung cancer by down-regulation of RAS, which results in suppression of both RAF/ERK and AKT signalling (Park *et al*. 2010).

Combination treatment with lovastatin and NVP-BEZ235 significantly increased apoptosis compared with single treatment with NVP-BEZ235 but slightly decreased apoptosis compared with lovastatin treatment alone. Thus, inhibition of ERK appears to specifically increase apoptosis. However, the observed decrease in MPC and MTTcell viability after

single NVP-BEZ235 treatment does not seem to be due to apoptosis induction. Apoptosis induction is likely to be prevented by an escape mechanism via ERK up-regulation after single treatment with NVP-BEZ235. Therefore, the observed effect of less apoptosis induction after combination treatment compared with single lovastatin treatment may be partly due to a higher remaining ERK activity after combination treatment compared with single lovastatin treatment and possibly the enhanced cytostatic effects after additional NVP-BEZ235 treatment render cells less sensitive to pro-apoptotic stimuli. The combination treatment of lovastatin with NVP-BEZ235 markedly increased the inhibitory effect on the cell cycle with an induction of G1 arrest compared with each drug separately. This makes the idea of combination treatment with low doses of NVP-BEZ235 and lovastatin even more interesting as a therapeutic manipulation. Accordingly, combination treatment with 10 μM lovastatin plus 50 nM NVP-BEZ235 reduced cell viability more effectively than single treatment with 10 μM lovastatin alone (by 95 vs 75% in MPC cells, by 77 vs 54% in MTT cells) and also decreased cell viability more potently than single treatment with 50 nM NVP-BEZ235 (by 95 vs 78% in MPC cells, by 77 vs 54% in MTT cells).

Comparison of MPC and MTT cells

Both cell lines showed broadly similar responses to all drugs tested. Lovastatin-induced apoptosis (caspase-3/7 activation) was slightly stronger in MTT than in MPC cells compared with the vehicle, which may be due to a higher requirement of mevalonate-derived isoprenoids in malignant cells compared with benign cells because of higher HMG-CoA expression (Hentosh *et al*. 2001; see also under Discussion, ‘Lovastatin as an ERK inhibitor’).

Conclusions

Several possible ‘mechanisms of resistance’ to different drugs have been observed in PCC cells in this study: PI3K/AKT inhibition by NVP-AEW541 was accompanied by ERK and mTORC1/p70S6K activation, dual PI3K/mTORC1/2 inhibition by NVP-BEZ235 was associated with ERK activation and inhibition of both AKT and ERK by lovastatin was accompanied by mTORC1/p70S6K activation. Regarding these potential mechanisms of interaction between PI3K/AKT, RAS/RAF/ERK and mTORC1/p70S6K signalling, we speculated that inhibition of one or two of these pathways alone may be associated with the activation of the remaining ones. This, indeed, argues for a therapeutic approach that targets PI3K/AKT, mTORC1, mTORC2 and ERK at the same time, and we have shown that this is the case in these PCC cell lines. However, further *in vivo* studies will be necessary before the use of such combinations can be explored in clinical practice.

Acknowledgments

Funding

This work was supported by the German Research Foundation (grant number NO925/1-1).

The authors thank Novartis and the German Research Foundation (Deutsche Forschungsgemeinschaft, DFG).

References

Adjalle R, Plouin PF, Pacak K, Lehnert H. Treatment of malignant pheochromocytoma. Hormone and Metabolic Research. 2009; 41:687–696.10.1055/s-0029-1231025 [PubMed: 19672813]

Astuti D, Hart-Holden N, Latif F, Lalloo F, Black GC, Lim C, Moran A, Grossman AB, Hodgson SV, Freemont A, et al. Genetic analysis of mitochondrial complex II subunits SDHD, SDHB and SDHC in paraganglioma and phaeochromocytoma susceptibility. Clinical Endocrinology. 2003; 59:728–733.10.1046/j.1365-2265.2003.01914.x [PubMed: 14974914]

Baysal BE, Ferrell RE, Willett-Brozick JE, Lawrence EC, Myssiorek D, Bosch A, van der Mey A, Taschner PE, Rubinstein WS, Myers EN, et al. Mutations in SDHD, a mitochondrial complex II gene, in hereditary paraganglioma. Science. 2000; 287:848–851.10.1126/science.287.5454.848 [PubMed: 10657297]

Brachmann SM, Hofmann I, Schnell C, Fritsch C, Wee S, Lane H, Wang S, Garcia-Echeverria C, Maira SM. Specific apoptosis induction by the dual PI3K/mTor inhibitor NVP-BEZ235 in HER2 amplified and PIK3CA mutant breast cancer cells. PNAS. 2009; 106:22299–22304.10.1073/pnas.0905152106 [PubMed: 20007781]

Burnichon N, Briere JJ, Libe R, Vescovo L, Riviere J, Tissier F, Jouanno E, Jeunemaitre X, Benit P, Tzagoloff A, et al. SDHA is a tumor suppressor gene causing paraganglioma. Human Molecular Genetics. 2010; 19:3011–3020.10.1093/hmg/ddq206 [PubMed: 20484225]

Burnichon N, Vescovo L, Amar L, Libe R, De RA, Venisse A, Jouanno E, Laurendeau I, Parfait B, Bertherat J, et al. Integrative genomic analysis reveals somatic mutations in pheochromocytoma and paraganglioma. Human Molecular Genetics. 2011; 20:3974–3985.10.1093/hmg/ddr324 [PubMed: 21784903]

Cafforio P, Dammacco F, Gernone A, Silvestris F. Statins activate the mitochondrial pathway of apoptosis in human lymphoblasts and myeloma cells. Carcinogenesis. 2005; 26:883–891.10.1093/carcin/bgi036 [PubMed: 15705602]

Carracedo A, Pandolfi PP. The PTEN–PI3K pathway: of feedbacks and cross-talks. Oncogene. 2008; 27:5527–5541.10.1038/onc.2008.247 [PubMed: 18794886]

Carracedo A, Ma L, Teruya-Feldstein J, Rojo F, Salmena L, Alimonti A, Egia A, Sasaki AT, Thomas G, Kozma SC, et al. Inhibition of mTORC1 leads to MAPK pathway activation through a PI3K-dependent feedback loop in human cancer. Journal of Clinical Investigation. 2008; 118:3065–3074. [PubMed: 18725988]

Cemeus C, Zhao TT, Barrett GM, Lorimer IA, Dimitroulakos J. Lovastatin enhances gefitinib activity in glioblastoma cells irrespective of EGFRvIII and PTEN status. Journal of Neurooncology. 2008; 90:9–17.10.1007/s11060-008-9627-0

Comino-Mendez I, Gracia-Aznarez FJ, Schiavi F, Landa I, Leandro-Garcia LJ, Leton R, Honrado E, Ramos-Medina R, Caronia D, Pita G, et al. Exome sequencing identifies MAX mutations as a cause of hereditary pheochromocytoma. Nature Genetics. 2011; 43:663–667.10.1038/ng.861 [PubMed: 21685915]

Cook MR, Pinchot SN, Jaskula-Sztul R, Luo J, Kunnimalaiyaan M, Chen H. Identification of a novel RAF1 pathway activator that inhibits gastrointestinal carcinoid cell growth. Molecular Cancer Therapeutics. 2010; 9:429–437.10.1158/1535-7163.MCT-09-0718 [PubMed: 20103603]

Crick DC, Andres DA, Danesi R, Macchia M, Waechter CJ. Geranylgeraniol overcomes the block of cell proliferation by lovastatin in C6 glioma cells. Journal of Neurochemistry. 1998; 70:2397–2405.10.1046/j.1471-4159.1998.70062397.x [PubMed: 9603204]

Dahia PL, Hao K, Rogus J, Colin C, Pujana MA, Ross K, Magoffin D, Aronin N, Cascon A, Hayashida CY, et al. Novel pheochromocytoma susceptibility loci identified by integrative genomics. Cancer Research. 2005a; 65:9651–9658.10.1158/0008-5472.CAN-05-1427 [PubMed: 16266984]

Dahia PL, Ross KN, Wright ME, Hayashida CY, Santagata S, Barontini M, Kung AL, Sanso G, Powers JF, Tischler AS, et al. A HIF1α regulatory loop links hypoxia and mitochondrial signals in pheochromocytomas. PLoS Genetics. 2005b; 1:72–80.10.1371/journal.pgen.0010008 [PubMed: 16103922]

Demierre MF, Higgins PD, Gruber SB, Hawk E, Lippman SM. Statins and cancer prevention. Nature Reviews. Cancer. 2005; 5:930–942.10.1038/nrc1751 [PubMed: 16341084]

Dimitroulakos J, Lorimer IA, Goss G. Strategies to enhance epidermal growth factor inhibition: targeting the mevalonate pathway. Clinical Cancer Research. 2006; 12:4426s–4431s. 10.1158/1078-0432.CCR-06-0089 [PubMed: 16857822]

Druce MR, Kaltsas GA, Fraenkel M, Gross DJ, Grossman AB. Novel and evolving therapies in the treatment of malignant phaeochromocytoma: experience with the mTOR inhibitor everolimus (RAD001). Hormone and Metabolic Research. 2009; 41:697–702.10.1055/s-0029-1220687 [PubMed: 19424940]

Eisenhofer G, Huynh TT, Pacak K, Brouwers FM, Walther MM, Linehan WM, Munson PJ, Mannelli M, Goldstein DS, Elkahloun AG. Distinct gene expression profiles in norepinephrine- and epinephrine-producing hereditary andsporadic pheochromocytomas: activation of hypoxia-driven angiogenic pathways in von Hippel–Lindau syndrome. Endocrine-Related Cancer. 2004; 11:897–911.10.1677/erc.1.00838 [PubMed: 15613462]

Fassnacht M, Kreissl MC, Weismann D, Allolio B. New targets and therapeutic approaches for endocrine malignancies. Pharmacological Therapy. 2009; 123:117–141.10.1016/j.pharmthera.2009.03.013

Favier J, Gimenez-Roqueplo AP. Pheochromocytomas: the (pseudo)-hypoxia hypothesis. Best Practice & Research. Clinical Endocrinology & Metabolism. 2010; 24:957–968.10.1016/j.beem.2010.10.004 [PubMed: 21115164]

Follet J, Corcos L, Baffet G, Ezan F, Morel F, Simon B, Le Jossic-Corcos C. The association of statins and taxanes: an efficient combination trigger of cancer cell apoptosis. British Journal of Cancer. 2012; 106:685–692.10.1038/bjc.2012.6 [PubMed: 22294184]

Fottner C, Minnemann T, Kalmbach S, Weber MM. Over-expression of the insulin-like growth factor I receptor in human pheochromocytomas. Journal of Molecular Endocrinology. 2006; 36:279–287.10.1677/jme.1.01975 [PubMed: 16595699]

Grant S. Cotargeting survival signaling pathways in cancer. Journal of Clinical Investigation. 2008; 118:3003–3006.10.1172/JCI36898E1 [PubMed: 18725993]

Grogan RH, Mitmaker EJ, Duh QY. Changing paradigms in the treatment of malignant pheochromocytoma. Cancer Control. 2011; 18:104–112. [PubMed: 21451453]

Guan KL, Figueroa C, Brtva TR, Zhu T, Taylor J, Barber TD, Vojtek AB. Negative regulation of the serine/threonine kinase B-Raf by Akt. Journal of Biological Chemistry. 2000; 275:27354–27359.10.1074/jbc.M004371200 [PubMed: 10869359]

Hao HX, Khalimonchuk O, Schraders M, Dephoure N, Bayley JP, Kunst H, Devilee P, Cremers CW, Schiffman JD, Bentz BG, et al. SDH5, a gene required for flavination of succinate dehydrogenase, is mutated in paraganglioma. Science. 2009; 325:1139–1142.10.1126/science.1175689 [PubMed: 19628817]

Hentosh P, Yuh SH, Elson CE, Peffley DM. Sterol-independent regulation of 3-hydroxy-3-methylglutaryl coenzyme A reductase in tumor cells. Molecular Carcinogenesis. 2001; 32:154–166.10.1002/mc.1074 [PubMed: 11746827]

Holstein SA, Knapp HR, Clamon GH, Murry DJ, Hohl RJ. Pharmacodynamic effects of high dose lovastatin in subjects with advanced malignancies. Cancer Chemotherapy and Pharmacology. 2006; 57:155–164.10.1007/s00280-005-0013-8 [PubMed: 16133537]

Hopfner M, Baradari V, Huether A, Schofl C, Scherubl H. The insulin-like growth factor receptor 1 is a promising target for novel treatment approaches in neuroendocrine gastrointestinal tumours. Endocrine-Related Cancer. 2006; 13:135–149.10.1677/erc.1.01090 [PubMed: 16601284]

Hresko RC, Mueckler M. mTOR.RICTOR is the Ser473 kinase for Akt/protein kinase B in 3T3-L1 adipocytes. Journal of Biological Chemistry. 2005; 280:40406–40416.10.1074/jbc.M508361200 [PubMed: 16221682]

Iida S, Miki Y, Ono K, Akahira J, Nakamura Y, Suzuki T, Sasano H. Synergistic anti-tumor effects of RAD001 with MEK inhibitors in neuroendocrine tumors: a potential mechanism of therapeutic limitation of mTOR inhibitor. Molecular and Cellular Endocrinology. 2012; 350:99–106.10.1016/j.mce.2011.11.024 [PubMed: 22178087]

Jakobisiak M, Bruno S, Skierski JS, Darzynkiewicz Z. Cell cycle-specific effects of lovastatin. PNAS. 1991; 88:3628–3632.10.1073/pnas.88.9.3628 [PubMed: 1673788]

Joshua AM, Ezzat S, Asa SL, Evans A, Broom R, Freeman M, Knox JJ. Rationale and evidence for sunitinib in the treatment of malignant paraganglioma/pheochromocytoma. Journal of Clinical Endocrinology and Metabolism. 2009; 94:5–9.10.1210/jc.2008-1836 [PubMed: 19001511]

Kappes A, Vaccaro A, Kunnimalaiyaan M, Chen H. ZM336372, a RAF1 activator, inhibits growth of pheochromocytoma cells. Journal of Surgical Research. 2006; 133:42–45.10.1016/j.jss.2006.02.002 [PubMed: 16603190]

Kinkade CW, Castillo-Martin M, Puzio-Kuter A, Yan J, Foster TH, Gao H, Sun Y, Ouyang X, Gerald WL, Cordon-Cardo C, et al. Targeting AKT/mTOR and ERK MAPK signaling inhibits hormone-refractory prostate cancer in a preclinical mouse model. Journal of Clinical Investigation. 2008; 118:3051–3064.10.1172/JCI34764 [PubMed: 18725989]

Ladroue C, Carcenac R, Leporrier M, Gad S, Le HC, Galateau-Salle F, Feunteun J, Pouyssegur J, Richard S, Gardie B. PHD2 mutation and congenital erythrocytosis with paraganglioma. New England Journal of Medicine. 2008; 359:2685–2692.10.1056/NEJMoa0806277 [PubMed: 19092153]

Latif F, Tory K, Gnarra J, Yao M, Duh FM, Orcutt ML, Stackhouse T, Kuzmin I, Modi W, Geil L. Identification of the von Hippel–Lindau disease tumor suppressor gene. Science. 1993; 260:1317–1320.10.1126/science.8493574 [PubMed: 8493574]

Lee M, Theodoropoulou M, Graw J, Roncaroli F, Zatelli MC, Pellegata NS. Levels of p27 sensitize to dual PI3K/mTOR inhibition. Molecular Cancer Therapeutics. 2011; 10:1450–1459.10.1158/1535-7163.MCT-11-0188 [PubMed: 21646547]

Liu B, Yang P, Ye Y, Zhou Y, Li L, Tashiro S, Onodera S, Ikejima T. Role of ROS in the protective effect of silibinin on sodium nitroprusside-induced apoptosis in rat pheochromocytoma PC12 cells. Free Radical Research. 2011; 45:835–847.10.3109/10715762.2011.580343 [PubMed: 21568648]

Lopez-Jimenez E, Gomez-Lopez G, Leandro-Garcia LJ, Munoz I, Schiavi F, Montero-Conde C, de Cubas AA, Ramires R, Landa I, Leskela S, et al. Research resource: transcriptional profiling reveals different pseudohypoxic signatures in SDHB and VHL-related pheochromocytomas. Molecular Endocrinology. 2010; 24:2382–2391.10.1210/me.2010-0256 [PubMed: 20980436]

Ma Y, Liu W, Wang Y, Chao X, Qu Y, Wang K, Fei Z. VEGF protects rat cortical neurons from mechanical trauma injury induced apoptosis via the MEK/ERK pathway. Brain Research Bulletin. 2011; 86:441–446.10.1016/j.brainresbull.2011.07.007 [PubMed: 21801813]

Maltese WA, Sheridan KM. Differentiation of neuroblastoma cells induced by an inhibitor of mevalonate synthesis: relation of neurite outgrowth and acetylcholinesterase activity to changes in cell proliferation and blocked isoprenoid synthesis. Journal of Cellular Physiology. 1985; 125:540–558.10.1002/jcp.1041250326 [PubMed: 3851809]

Mantha AJ, Hanson JE, Goss G, Lagarde AE, Lorimer IA, Dimitroulakos J. Targeting the mevalonate pathway inhibits the function of the epidermal growth factor receptor. Clinical Cancer Research. 2005; 11:2398–2407.10.1158/1078-0432.CCR-04-1951 [PubMed: 15788691]

Marcelli M, Cunningham GR, Haidacher SJ, Padayatty SJ, Sturgis L, Kagan C, Denner L. Caspase-7 is activated during lovastatin-induced apoptosis of the prostate cancer cell line LNCaP. Cancer Research. 1998; 58:76–83. [PubMed: 9426061]

Martiniova L, Lai EW, Elkahloun AG, Abu-Asab M, Wickremasinghe A, Solis DC, Perera SM, Huynh TT, Lubensky IA, Tischler AS, et al. Characterization of an animal model of aggressive metastatic pheochromocytoma linked to a specific gene signature. Clinical and Experimental Metastasis. 2009; 26:239–250.10.1007/s10585-009-9236-0 [PubMed: 19169894]

Mulligan LM, Kwok JB, Healey CS, Elsdon MJ, Eng C, Gardner E, Love DR, Mole SE, Moore JK, Papi L. Germ-line mutations of the RET proto-oncogene in multiple endocrine neoplasia type 2A. Nature. 1993; 363:458–460.10.1038/363458a0 [PubMed: 8099202]

Niemann S, Muller U. Mutations in SDHC cause autosomal dominant paraganglioma, type 3. Nature Genetics. 2000; 26:268–270.10.1038/81551 [PubMed: 11062460]

Nölting S, Grossman AB. Signaling pathways in pheochromo-cytomas and paragangliomas: prospects for future therapies. Endocrine Pathology. 2012; 23:21–33.10.1007/s12022-012-9199-6 [PubMed: 22391976]

Olson MF, Paterson HF, Marshall CJ. Signals from Ras and Rho GTPases interact to regulate expression of p21Waf1/Cip1. Nature. 1998; 394:295–299.10.1038/28425 [PubMed: 9685162]

O'Reilly KE, Rojo F, She QB, Solit D, Mills GB, Smith D, Lane H, Hofmann F, Hicklin DJ, Ludwig DL, et al. mTOR inhibition induces upstream receptor tyrosine kinase signaling and activates Akt. Cancer Research. 2006; 66:1500–1508.10.1158/0008-5472.CAN-05-2925 [PubMed: 16452206]

Park C, Lee I, Kang WK. Lovastatin-induced E2F-1 modulation and its effect on prostate cancer cell death. Carcinogenesis. 2001; 22:1727–1731.10.1093/carcin/22.10.1727 [PubMed: 11577016]

Park KS, Lee JL, Ahn H, Koh JM, Park I, Choi JS, Kim YR, Park TS, Ahn JH, Lee DH, et al. Sunitinib, a novel therapy for anthracycline- and cisplatin-refractory malignant pheochromocytoma. Japanese Journal of Clinical Oncology. 2009; 39:327–331.10.1093/jjco/hyp005 [PubMed: 19264767]

Park IH, Kim JY, Jung JI, Han JY. Lovastatin overcomes gefitinib resistance in human non-small cell lung cancer cells with K-Ras mutations. Investigational New Drugs. 2010; 28:791–799.10.1007/s10637-009-9319-4 [PubMed: 19760159]

Powers JF, Evinger MJ, Tsokas P, Bedri S, Alroy J, Shahsavari M, Tischler AS. Pheochromocytoma cell lines from heterozygous neurofibromatosis knockout mice. Cell and Tissue Research. 2000; 302:309–320.10.1007/s004410000290 [PubMed: 11151443]

Powers JF, Evinger MJ, Zhi J, Picard KL, Tischler AS. Pheochromocytomas in Nf1 knockout mice express a neural progenitor gene expression profile. Neuroscience. 2007; 147:928–937.10.1016/j.neuroscience.2007.05.008 [PubMed: 17582688]

Qin Y, Yao L, King EE, Buddavarapu K, Lenci RE, Chocron ES, Lechleiter JD, Sass M, Aronin N, Schiavi F, et al. Germline mutations in TMEM127 confer susceptibility to pheochromocytoma. Nature Genetics. 2010; 42:229–233.10.1038/ng.533 [PubMed: 20154675]

Rao S, Porter DC, Chen X, Herliczek T, Lowe M, Keyomarsi K. Lovastatin-mediated G1 arrest is through inhibition of the proteasome, independent of hydroxymethyl glutaryl-CoA reductase. PNAS. 1999; 96:7797–7802.10.1073/pnas.96.14.7797 [PubMed: 10393901]

Ricciardi MR, Scerpa MC, Bergamo P, Ciuffreda L, Petrucci MT, Chiaretti S, Tavolaro S, Mascolo MG, Abrams SL, Steelman LS, et al. Therapeutic potential of MEK inhibition in acute myelogenous leukemia: rationale for "vertical" and "lateral" combination strategies. Journal of Molecular Medicine. 2012 In press.

Santarpia L, Habra MA, Jimenez C. Malignant pheochromocytomas and paragangliomas: molecular signaling pathways and emerging therapies. Hormone and Metabolic Research. 2009; 41:680–686.10.1055/s-0029-1214381 [PubMed: 19343618]

Schlisio S, Kenchappa RS, Vredeveld LC, George RE, Stewart R, Greulich H, Shahriari K, Nguyen NV, Pigny P, Dahia PL, et al. The kinesin KIF1Bβ acts downstream from EglN3 to induce apoptosis and is a potential 1p36 tumor suppressor. Genes and Development. 2008; 22:884–893.10.1101/gad.1648608 [PubMed: 18334619]

Serra V, Markman B, Scaltriti M, Eichhorn PJ, Valero V, Guzman M, Botero ML, Llonch E, Atzori F, Di CS, et al. NVP-BEZ235, a dual PI3K/mTOR inhibitor, prevents PI3K signaling and inhibits the growth of cancer cells with activating PI3K mutations. Cancer Research. 2008; 68:8022–8030.10.1158/0008-5472.CAN-08-1385 [PubMed: 18829560]

Serra V, Scaltriti M, Prudkin L, Eichhorn PJ, Ibrahim YH, Chandarlapaty S, Markman B, Rodriguez O, Guzman M, Rodriguez S, et al. PI3K inhibition results in enhanced HER signaling and acquired ERK dependency in HER2-overexpressing breast cancer. Oncogene. 2011; 30:2547–2557.10.1038/onc.2010.626 [PubMed: 21278786]

Sippel RS, Chen H. Activation of the ras/RAF1 signal transduction pathway in carcinoid tumor cells results in morphologic transdifferentiation. Surgery. 2002; 132:1035–1039.10.1067/msy.2002.128877 [PubMed: 12490852]

Sippel RS, Carpenter JE, Kunnimalaiyaan M, Chen H. The role of human achaete-scute homolog-1 in medullary thyroid cancer cells. Surgery. 2003a; 134:866–871.10.1016/S0039-6060(03)00418-5 [PubMed: 14668716]

Sippel RS, Carpenter JE, Kunnimalaiyaan M, Lagerholm S, Chen H. RAF1 activation suppresses neuroendocrine marker and hormone levels in human gastrointestinal carcinoid cells. American

Journal of Physiology. Gastrointestinal and Liver Physiology. 2003b; 285:G245–G254.10.1152/ajpgi.00420.2002 [PubMed: 12851216]

Steelman LS, Abrams SL, Whelan J, Bertrand FE, Ludwig DE, Basecke J, Libra M, Stivala F, Milella M, Tafuri A, et al. Contributions of the Raf/MEK/ERK, PI3K/PTEN/Akt/mTOR and Jak/STAT pathways to leukemia. Leukemia. 2008; 22:686–707.10.1038/leu.2008.26 [PubMed: 18337767]

Subbiah V, Naing A, Brown RE, Chen H, Doyle L, LoRusso P, Benjamin R, Anderson P, Kurzrock R. Targeted morphoproteomic profiling of Ewing's sarcoma treated with insulin-like growth factor 1 receptor (IGF1R) inhibitors: response/resistance signatures. PLoS ONE. 2011; 6:e18424.10.1371/journal.pone.0018424 [PubMed: 21494688]

Ukomadu C, Dutta A. p21-dependent inhibition of colon cancer cell growth by mevastatin is independent of inhibition of G1 cyclin-dependent kinases. Journal of Biological Chemistry. 2003; 278:43586–43594.10.1074/jbc.M307194200 [PubMed: 12930830]

Vaccaro A, Chen H, Kunnimalaiyaan M. *In-vivo* activation of RAF1 inhibits tumor growth and development in a xenograft model of human medullary thyroid cancer. Anticancer Drugs. 2006; 17:849–853.10.1097/01.cad.0000217424.36961.47 [PubMed: 16926634]

Van Gompel JJ, Kunnimalaiyaan M, Holen K, Chen H. ZM336372, a RAF1 activator, suppresses growth and neuroendo-crine hormone levels in carcinoid tumor cells. Molecular Cancer Therapeutics. 2005; 4:910–917.10.1158/1535-7163.MCT-04-0334 [PubMed: 15956248]

Viskochil D, Buchberg AM, Xu G, Cawthon RM, Stevens J, Wolff RK, Culver M, Carey JC, Copeland NG, Jenkins NA. Deletions and a translocation interrupt a cloned gene at the neurofibromatosis type 1 locus. Cell. 1990; 62:187–192.10.1016/0092-8674(90)90252-A [PubMed: 1694727]

Whyte DB, Kirschmeier P, Hockenberry TN, Nunez-Oliva I, James L, Catino JJ, Bishop WR, Pai JK. K- and N-Ras are geranylgeranylated in cells treated with farnesyl protein transferase inhibitors. Journal of Biological Chemistry. 1997; 272:14459–14464.10.1074/jbc.272.22.14459 [PubMed: 9162087]

von Wichert G, Jehle PM, Hoeflich A, Koschnick S, Dralle H, Wolf E, Wiedenmann B, Boehm BO, Adler G, Seufferlein T. Insulin-like growth factor-I is an autocrine regulator of chromogranin A secretion and growth in human neuroendocrine tumor cells. Cancer Research. 2000; 60:4573–4581. [PubMed: 10969809]

Wong WW, Dimitroulakos J, Minden MD, Penn LZ. HMG-CoA reductase inhibitors and the malignant cell: the statin family of drugs as triggers of tumor-specific apoptosis. Leukemia. 2002; 16:508–519.10.1038/sj.leu.2402476 [PubMed: 11960327]

Wu J, Wong WW, Khosravi F, Minden MD, Penn LZ. Blocking the Raf/MEK/ERK pathway sensitizes acute myelogenous leukemia cells to lovastatin-induced apoptosis. Cancer Research. 2004; 64:6461–6468.10.1158/0008-5472.CAN-04-0866 [PubMed: 15374955]

Yeh IT, Lenci RE, Qin Y, Buddavarapu K, Ligon AH, Leteurtre E, Do CC, Cardot-Bauters C, Pigny P, Dahia PL. A germline mutation of the KIF1Bβ gene on 1p36 in a family with neural and nonneural tumors. Human Genetics. 2008; 124:279–285.10.1007/s00439-008-0553-1 [PubMed: 18726616]

Zhao TT, Trinh D, Addison CL, Dimitroulakos J. Lovastatin inhibits VEGFR and AKT activation: synergistic cytotoxicity in combination with VEGFR inhibitors. PLoS ONE. 2010; 5:e12563.10.1371/journal.pone.0012563 [PubMed: 20838437]

Zimmermann S, Moelling K. Phosphorylation and regulation of Raf by Akt (protein kinase B). Science. 1999; 286:1741–1744.10.1126/science.286.5445.1741 [PubMed: 10576742]

Zitzmann K, Ruden J, Brand S, Goke B, Lichtl J, Spottl G, Auernhammer CJ. Compensatory activation of Akt in response to mTOR and Raf inhibitors – a rationale for dual-targeted therapy approaches in neuroendocrine tumor disease. Cancer Letters. 2010; 295:100–109.10.1016/j.canlet.2010.02.018 [PubMed: 20356670]

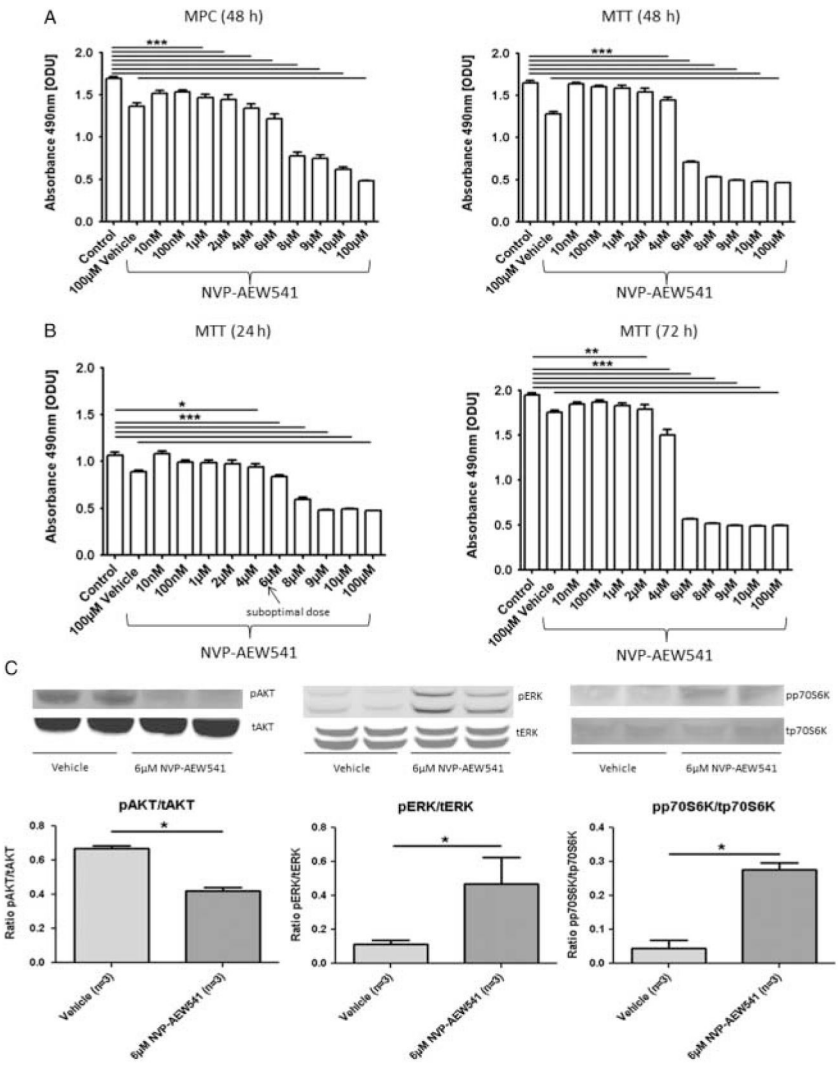

Figure 1.

NVP-AEW541. Cell viability after treatment with different concentrations of NVP-AEW541 was assessed by the MTS cell viability assay. MTS assay results are shown as ODU (mean±S.E.M.), which are linearly correlated with the cell number (R^2=0·97). (A) There was a dose-dependent decrease in cell viability in MPC and MTT cells after 48 h treatment with NVP-AEW541 (MPC (48 h): ODU: control (*n*=8) vs ≥1 µM NVP-AEW541 (*n*=8 for each condition), ***P≤0·001; MTT (48 h): ODU: control (*n*=8) vs ≥4 µM NVP-AEW541 (*n*=8 for each condition), ***P≤0·001; 100 µM vehicle: 1% DMSO). (B) The time-dependent effect of NVP-AEW541 in MTT cells: 4 µM NVP-AEW541 and higher concentrations significantly reduced MTT cell viability after 24 h treatment (*n*=8 for each condition, *P≤0·05, ***P≤0·001): 50% of this dose (2 µM) and higher doses significantly reduced MTT cell viability after 72 h treatment (*n*=8 for each condition, **P≤0·01, ***P≤0·001). (C) Phospho (p-) and total (t) protein expressions of AKT, ERK and p70S6K after treatment with suboptimal doses of NVP-AEW541 assessed by western blotting. The relative expression of each p-protein was calculated as the ratio of p-/t protein: 24 h

treatment of MTT cells with 6 μM NVP-AEW541 significantly decreased pAKT levels but significantly increased pERK and pp70S6K levels compared with the vehicle (ratio pAKT/tAKT, ratio pERK/tERK, ratio pp70S6K/tp70S6K: vehicle (n=3) vs 6 μM NVP-AEW541 (n=3), *P≤0·05).

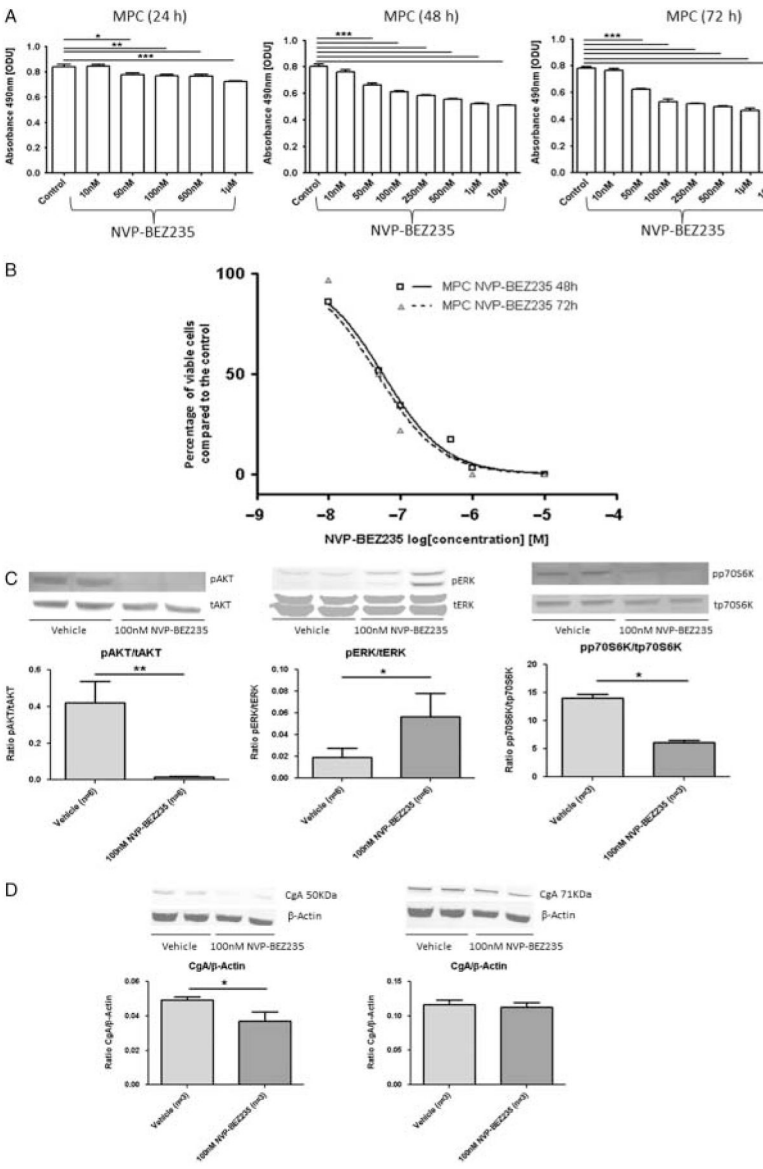

Figure 2.

NVP-BEZ235. Cell viability after treatment with different concentrations of NVP-BEZ235 was assessed by the MTS cell viability assay. MTS assay results are shown as ODU (mean ±S.E.M.), which are linearly correlated with the cell number (R^2=0·97) (A), and as the percentage of viable cells (mean±S.E.M.) compared with the control (B). (A) There was a dose- and time-dependent decrease in MPC cell viability after treatment with NVP-BEZ235. Treatment for 24, 48 and 72 h with 50 nM or higher concentrations of NVP-BEZ235 significantly decreased MPC cell viability compared with the control (MPC (24 h): ODU: control (*n*=8) vs 50 nM NVP-BEZ235 (*n*=8), **P*≤0·05; control (*n*=8) vs ≥100 nM NVP-BEZ235 (*n*=8 for each condition), ***P*≤0·01; control (*n*=8) vs 1 µM NVP-BEZ235 (*n*=8), ****P*≤0·001; MPC (48 and 72 h): ODU: control (*n*=8) vs ≥50 nM NVP-BEZ235 (*n*=8 for each condition), ****P*≤0·001). (B) MPC cell viability curves for 48 and 72 h treatment with NVP-BEZ235 (*n*=8 for each condition). The *x*-axis shows the drug concentrations as

log[M] : 48 h treatment with 1 and 10 μM NVP-BEZ235 decreased MPC cell viability by 96 and 100%, respectively, compared with the control ($P \leq 0{\cdot}001$); 72 h treatment with 1 and 10 μM NVP-BEZ235 reduced MPC cell viability by 100% compared with the control ($P \leq 0{\cdot}001$). (C) Phospho (p-) and total (t) protein expression of AKT, ERK and p70S6K after treatment with NVP-BEZ235 assessed by western blotting. The relative expression of each p-protein was calculated as the ratio of p-/t protein: 24 h treatment of MPC cells with 100 nM NVP-BEZ235 significantly diminished pAKT and pp70S6K levels but significantly increased pERK levels compared with the vehicle (ratio pAKT/tAKT: vehicle (n=6) vs 100 nM NVP-BEZ235 (n=6), $^{**}P \leq 0{\cdot}01$; ratio pERK/tERK: vehicle (n=6) vs 100 nM NVP-BEZ235 (n=6), $^{*}P \leq 0{\cdot}05$; ratio pp70S6K/tp70S6K: vehicle (n=3) vs 100 nM NVP-BEZ235 (n=3), $^{*}P \leq 0{\cdot}05$). (D) CgA expression assessed by western blotting. The relative expression of CgA was calculated as the ratio of CgA/β-actin: 24 h treatment of MPC cells with 100 nM NVP-BEZ235 significantly decreased the 50 kDa fragment of CgA compared with the vehicle (left panel, ratio CgA/β-actin: vehicle (n=3) vs 100 nM NVP-BEZ235 (n=3), $^{*}P \leq 0{\cdot}05$) while the 71 kDa fragment of CgA (right panel, ratio CgA/β-actin: vehicle (n=3) vs 100 nM NVP-BEZ235 (n=3), P=0·2) remained constant.

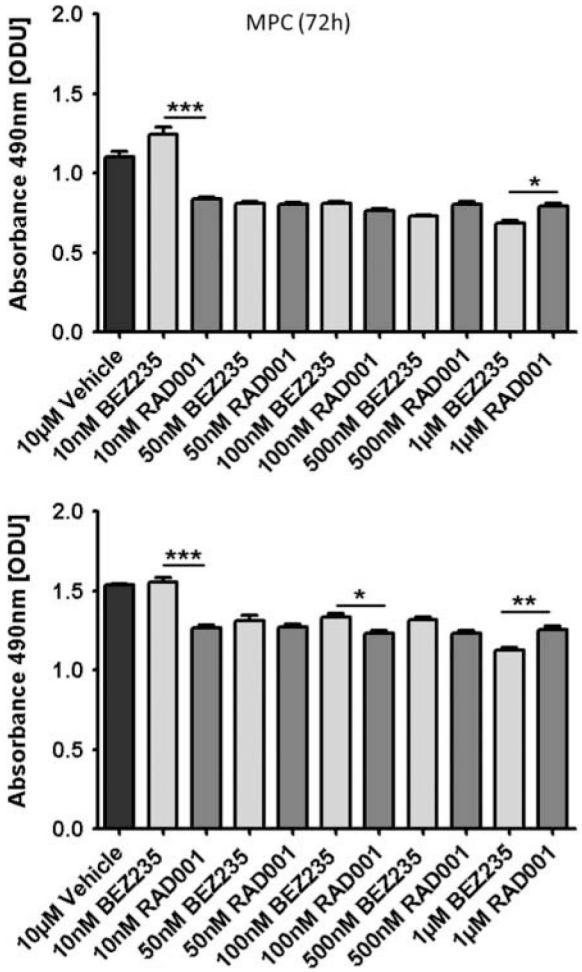

Figure 3.

NVP-BEZ235 vs everolimus (RAD001). MTS assay results are shown as ODU (mean ±S.E.M.), which are linearly correlated with the cell number (R^2=0·97). At higher doses (1 µM), NVP-BEZ235 showed significantly higher efficacy than everolimus (RAD001) in both cell lines. At lower doses (50–500 nM), both drugs showed similar efficacy in both cell lines. At very low doses (10 nM), everolimus was more effective than NVP-BEZ235 (n=8 for each condition, *P≤0·05, **P≤0·01 and ***P≤0·001).

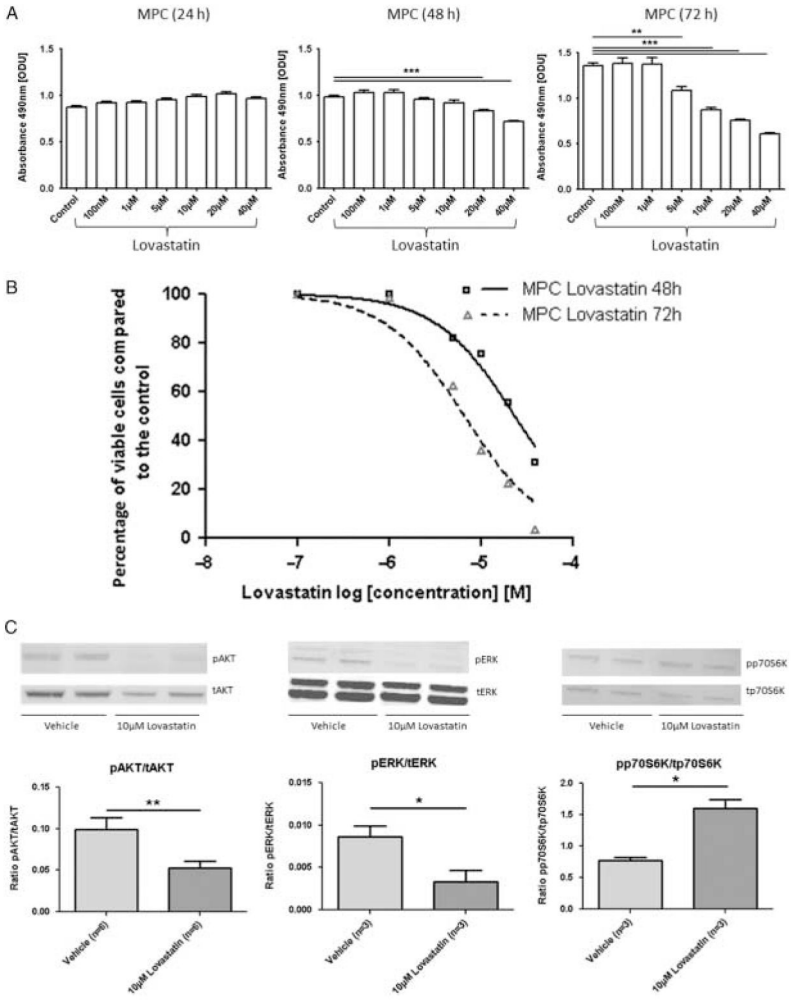

Figure 4.

Lovastatin. Cell viability after treatment with different concentrations of lovastatin was assessed by the MTS cell viability assay. MTS assay results are shown as ODU (mean ±S.E.M.), which are linearly correlated with the cell number (R^2=0·97) (A) and as percentage of viable cells (mean±S.E.M.) compared with the control (B). (A) There was a dose- and time-dependent decrease in MPC cell viability after lovastatin treatment: 24 h treatment did not affect cell viability; 48 h treatment with 20 µM and 72 h treatment with 5 µM or higher concentrations of lovastatin significantly decreased MPC cell viability (n=8 for each condition, **P≤0·01, ***P≤0·001). (B) MPC cell viability curves for 48 and 72 h treatment with lovastatin compared with the control (n=8 for each condition). The x-axis shows the drug concentrations as log[M]. Treatment with 40 µM lovastatin for 48 and 72 h decreased MPC cell viability by 69 and 96%, respectively, compared with the control (P≤0·001). Doses higher than 40 µM could not be applied to the cells because the lovastatin crystallised in FBS-containing media and was therefore cytotoxic. (C) Phospho (p-) and total (t) protein expression of AKT, ERK and p70S6K after treatment with lovastatin assessed by western blotting. The relative expression of each p-protein was calculated as the ratio of p-/t protein: 72 h treatment of MPC cells with 10 µM lovastatin significantly decreased pAKT

and pERK but significantly increased pp70S6K compared with the vehicle (ratio pAKT/tAKT: vehicle (n=6) vs 10 μM lovastatin (n=6), $^{**}P \leq 0{\cdot}01$; ratio pERK/tERK, ratio pp70S6K/tp70S6K: vehicle (n=3) vs 10 μM lovastatin (n=3), $^{*}P \leq 0{\cdot}05$).

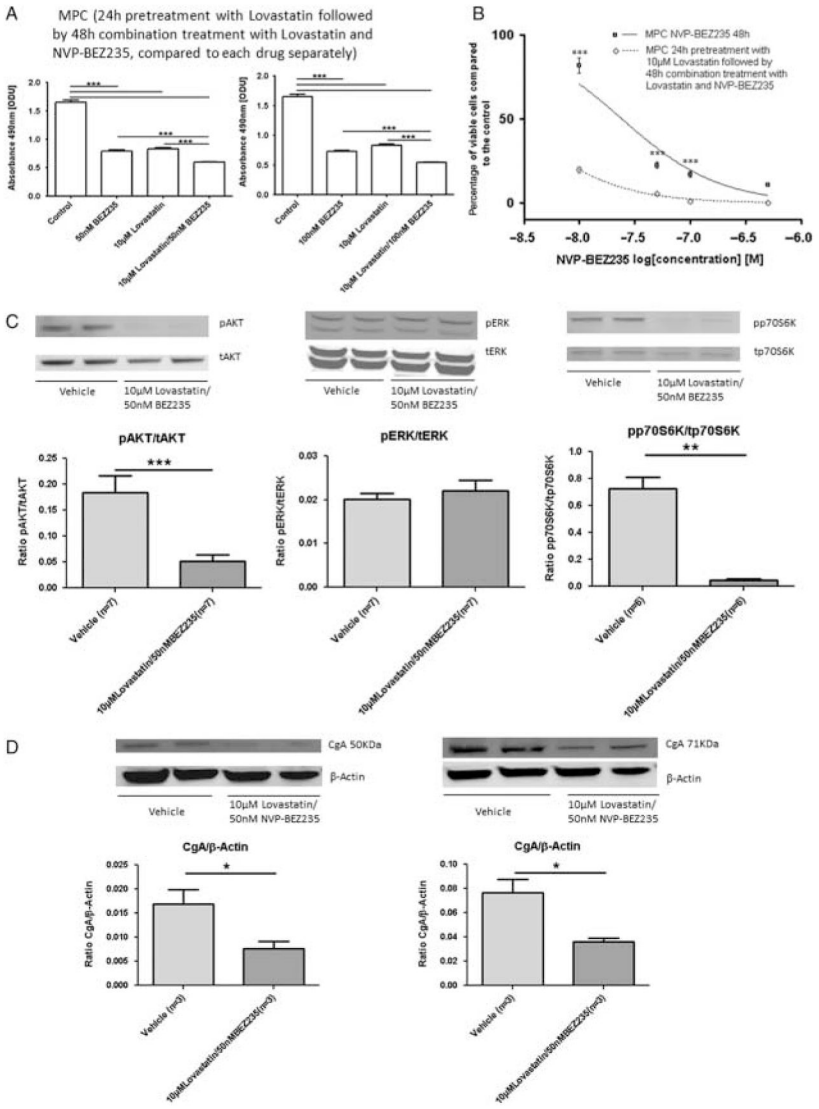

Figure 5.

Combination treatment with lovastatin and NVP-BEZ235. Cell viability after 24 h pretreatment with 10 μM lovastatin followed by 48 h combination treatment with 10 μM lovastatin and different concentrations of NVP-BEZ235 were assessed by the MTS cell viability assay. MTS assay results are shown as ODU (mean±S.E.M.), which are linearly correlated with the cell number (R^2=0·97) (A), and as the percentage of viable cells (mean ±S.E.M.) compared with the control (B). (A) 48 h combination treatment with NVP-BEZ235 and lovastatin after 24 h pretreatment with lovastatin reduced cell viability significantly more effectively than each drug separately (n=8 for each condition, ***P≤0·001). (B) MPC cell viability curves for 48 h treatment with NVP-BEZ235 alone and for 24 h pretreatment with lovastatin followed by 48 h combination treatment with NVP-BEZ235 and lovastatin (n=8 for each condition, ***P≤0·001). The x-axis shows the drug concentrations as log[M]: 48 h single treatment with 50 and 100 nM NVP-BEZ235 reduced MPC cell viability by 77 and 83%, respectively, compared with the control; 48 h treatment

with 50 and 100 nM NVP-BEZ235 in combination with 10 μM lovastatin decreased MPC cell viability by 95 and 99%, respectively, compared with the control. Not shown in this figure, 72 h single treatment with 10 μM lovastatin reduced MPC cell viability by 74% compared with the control. (C) Phospho (p-) and total (t) protein expression of AKT, ERK and p70S6K assessed by western blotting. The relative expression of each p-protein was calculated as the ratio of p-/t protein. The combination of 10 μM lovastatin with 50 nMNVP-BEZ235 for 24 h after 48 h pretreatment with 10 μM lovastatin significantly diminished pAKT and pp70S6K in MPC cells compared with the vehicle and prevented the pERK up-regulation induced by single NVP-BEZ235 treatment (ratio pAKT/tAKT: vehicle (n=7) vs 10 μM lovastatin plus 50 nM NVP-BEZ235 (n=7), ***P≤0·001; ratio pERK/tERK: vehicle (n=7) vs 10 μM lovastatin plus 50 nM NVP-BEZ235 (n=7), P=0·355; ratio pp70S6K/tp70S6K: vehicle (n=6) vs 10 μM lovastatin plus 50 nM NVP-BEZ235 (n=6), **P≤0·01). (D) CgA expression after 48 h pretreatment with 10 μM lovastatin followed by 24 h combination treatment with 10 μM lovastatin and 50 nM NVP-BEZ235 assessed by western blotting. The relative expression of CgA was calculated as the ratio of CgA/β-actin. The combination treatment significantly diminished both the 50 kDa fragment of CgA (left panel, ratio CgA/β-actin: vehicle (n=3) vs 10 μM lovastatin plus 50 nM NVP-BEZ235 (n=3), *P≤0·05) and the 71 kDa fragment of CgA (right panel, ratio CgA/β-actin: vehicle (n=3) vs 10 μM lovastatin plus 50 nM NVP-BEZ235 (n=3), *P≤0·05) compared with the vehicle in MPC cells.

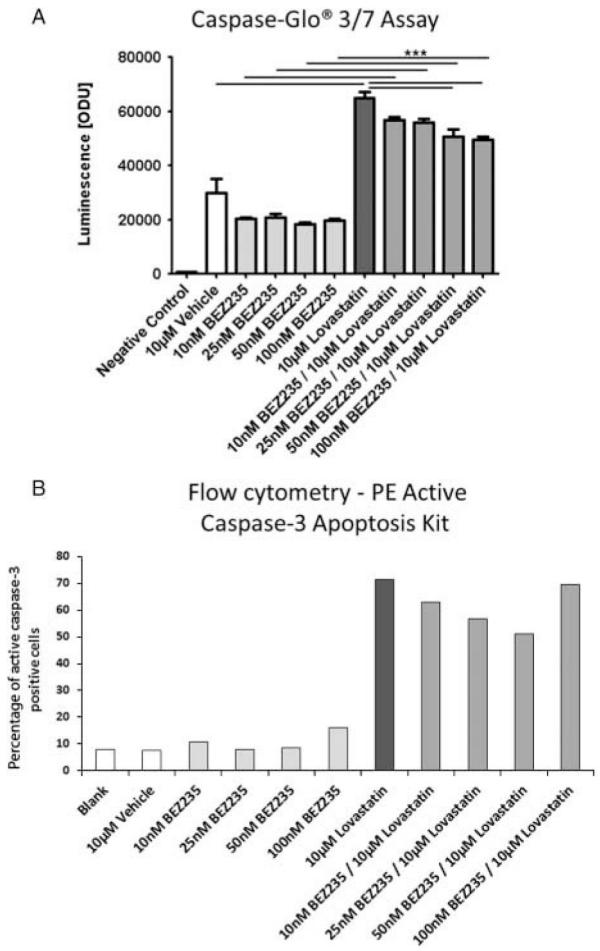

Figure 6.

Assessment of apoptosis. (A) Caspase-Glo 3/7 assay results are shown as ODU (mean ±S.E.M.). Treatment with NVP-BEZ235 alone did not induce apoptosis compared with the vehicle in MTT cells; treatment with lovastatin alone significantly increased apoptosis compared with the vehicle. After combination treatment, apoptosis was decreased progressively with increasing doses (10–100 nM) of NVP-BEZ235 compared with lovastatin alone but increased compared with NVP-BEZ235 alone (n=8 for each condition, ***$P \leq 0{\cdot}001$; negative control: no cells; 10 µM vehicle: 0·1% DMSO). (B) The results of the Caspase-Glo 3/7 assay were confirmed by flow cytometry using the PE Active Caspase-3 Apoptosis Kit to analyse the active caspase-3-positive cells. NVP-BEZ235 separately did not induce apoptosis compared with the vehicle. Lovastatin separately markedly induced apoptosis compared with the vehicle. The combination treatment slightly decreased apoptosis compared with single treatment with lovastatin but increased apoptosis compared with single treatment with NVP-BEZ235 (10 µM vehicle: 0·1% DMSO).

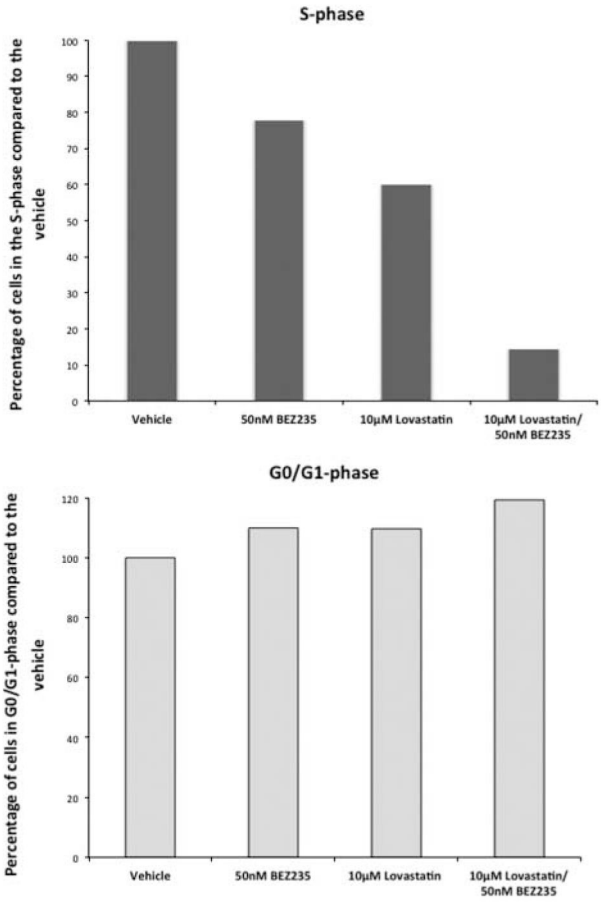

Figure 7.

Cell cycle. Cell cycle analysis was performed by flow cytometry. NVP-BEZ235 and lovastatin separately decreased the percentage of cells in the S-phase with a much stronger effect after combination treatment and concomitantly increased the percentage of cells in the G0/G1 phase.

Table 1

Antibodies used for western blotting in the current study

Antibody name	Origin	Concentration	Source	Primary/secondary	Monoclonal/polyclonal
Anti phospho-AKT (Ser473), #4051	Mouse	1:1000	Cell Signaling Technology, New England Biolabs, Hertfordshire, UK	Primary	Monoclonal
Anti-AKT (total), #9272	Rabbit	1:1000	Cell Signaling Technology, New England Biolabs	Primary	Polyclonal
Anti-diphospho-ERK-1 and 2, #M8159	Mouse	1:5000	Sigma, St. Louis, MO, USA	Primary	Monoclonal
Anti-ERK-1 and 2 (total), #M5670	Rabbit	1:5000	Sigma	Primary	Polyclonal
Anti-phospho-p70 S6 kinase (Thr389), #9206	Mouse	1:1000	Cell Signaling Technology, New England Biolabs	Primary	Monoclonal
Anti-p70S6 kinase (total), #9202	Rabbit	1:1000	Cell Signaling Technology, New England Biolabs	Primary	Polyclonal
Anti-chromogranin A, #ab15160	Rabbit	1:100	Abcam, Cambridge, UK	Primary	Polyclonal
Anti-beta actin antibody, #ab6276	Mouse	1:5000	Abcam	Primary	Monoclonal
Anti-rabbit IRDye_800, #611-132-002	Goat	1:5000	LI-COR Biosciences, Cambridge, UK	Secondary	Polyclonal
Anti-mouse IRDye_680, #926-32220	Goat	1:5000	LI-COR Biosciences	Secondary	Polyclonal